BACHELOR' S THESIS / BIOMEDICAL ENGINEERING 2023

Simulating the influence of proteoglycans changes in intervertebral disc mechanical behaviour

Inés Blanco Villaverde

upf. Universitat Pompeu Fabra Barcelona

Simulating the influence of proteoglycans changes in intervertebral disc mechanical behaviour

A bottom-up approach integrating cellular-level activity and tissue-level mechanics.

Inés Blanco Villaverde

Bachelor's thesis UPF 2022/2023

Thesis supervisor(s):

Dr. Carlos Eduardo Ruiz Wills

Barcelona Centre for New Medical Technologies

Biomechanics and Mechanobiology (BMMB)

Department of Information and Communications Technologies

Universitat Pompeu Fabra Barcelona

Acknowledgments

I would like to thank my supervisor, Carlos Ruiz Wills, for his commitment, support, and patience through this journey. He has not only fostered my intellectual growth but also valued and encouraged my ideas. I would also like to thank my family and friends for their support and love, a constant source of motivation.

Summary/Abstract

Around 80% of world population will suffer of low back pain (LBP). Such condition is often related with intervertebral disc (IVD) degeneration (DD). In DD, the proteoglycan (PG) loss is highly important since it compromises IVD response under compressive loads. DD has been studied using numerical models. Most of them address how mechanical loads affect nutrition and cells. Yet, no model has studied how extracellular matrix (ECM) changes affect disc mechanical response. Hence, the aim of this thesis is to study how PG changes can affect IVD mechanical behaviour. A novel 3D mechano-transport model of the L4-L5 IVD is used, incorporating a novel approach for fixed charged density (FCD) that considers nutrition-dependent PG dynamics. Simulations under physiological loads are performed for both non-degenerated and degenerated tissue conditions. FCD decrease, related to PG loss, significant impacts intradiscal pressure (IDP) but has minimal effect on disc height. This study shed light into the intricate relationship between ECM changes, disc degeneration and mechanical response, providing foundation for future research.

Keywords

Intervertebral disc degeneration, biochemical changes, Finite element analysis, Proteoglycans, Mechanical behaviour.

Preface or prologue

If someone had told me in the first years of this degree that my thesis was going to be in the field of biomechanics, I probably would not have believed it. I come from a small high school in Asturias, where there were not enough students to study physics. So, my initial encounters with biomechanics were complicated.

It was through my growing interest in software management and programming that in the course of numerical methods, taught by Carlos, I began to understand the potential of computer simulations and finite element models, my first contact with Abaqus. I did my internship in the Biomechanics and Mechanobiology group, under the guidance of Carlos. His passion for sharing his knowledge made it a fundamental experience, completely changing my perspective on biomechanics, understanding the power of combining it with FE models, being able to study and solve a real complex problem in a virtual way, incredible.

One of the projects that Carlos offered me to my thesis was the development of a comprehensive FE approach to study intervertebral disc degeneration, with the aim of understanding the influence of proteoglycans, essential proteins in intervertebral discs, on the disc mechanical behaviour, and provide valuable information to the prevalent condition of low back pain, a challenge I accepted.

They were 9 months of learning, where we fostered open communication and imagination to overcome all obstacles, where Carlos taught me the value of patience.

In this thesis, you will witness the importance of collaboration, determination, and passion, transmitted by Carlos, to produce, what I feel is, a valuable work. I am proud to say that this thesis is not only the end of my career, but also the beginning of new possibilities and future research.

Index

List of figures

List of tables

1 Introduction

1.1 Problem and motivation

Low back pain (LBP) is a highly prevalent condition affecting individuals worldwide, causing a significant socio-economic burden. It is estimated that up to 80% of the population will experience LBP at some point in their life (Hoy et al., 2012). Among the factors contributing to LBP, intervertebral disc (IVD) degeneration is a major cause (Huang, Y. C, et al., 2014), and its associated pain can severely impair patient's quality of life. The prevalence of LBP is expected to increase due to aging population and the rise in sedentary lifestyle (Baradaran Mahdavi, S., et al., 2021). Therefore, the study of IVD degeneration is essential to understand the pathophysiology of LBP.

IVD is a complex avascular structure, responsible for the functional articulation of the spine, playing a significant role on its support, stability, and flexibility (Huang, Y. C, et al., 2014). Disc degeneration (DD) is a complex process characterized by biochemical and structural changes in the disc's extracellular matrix (ECM), which lead to its altered mechanical response (Smith L.J., et al., 2011). Nutrition is vital to the disc due to its avascularity, and any disruption to this process can affect ECM homeostasis, which in turn affects the ability of the disc to respond to mechanical loads and stresses and compromise the production of proteoglycans (PG) (Urban and Roberts, 2003; Rajasekaran et al., 2008; Vergroesen et al., 2015; Baumgartner et al., 2020).

Among the key biochemical changes observed in degenerated IVDs, PG loss has been identified as a remarkable phenomenon that alters the mechanical properties of the tissue and contributes to the degenerative cascade (Urban & Roberts, 2003; Kos, N., et al., 2019; Huang, Y. C, et al., 2014). PGs are large, complex molecules that play a crucial role in maintaining the structure and function of the ECM and that are responsible for the high osmotic pressure and swelling of the nucleus (Urban & McMullin, 1985), which contribute to the tissue's ability to resist compressive loads (Urban and Roberts, 2003; Iatridis et al., 2013). The osmotic pressure primarily relies on the concentration of fixed negative charges present on the proteoglycans, which is referred to as the fixed charge density (FCD) (Urban, J. P., & McMullin, J. F., 1985).

Various approaches, including experimental studies and in silico models, are used to study DD. Experimental studies have provided crucial insights into tissue composition and the impact of disrupted nutrition (Rinkler et al. 2010; Horner & Urban 2001; Bibby et al., 2005; Vo, N. et al., 2010; Neidlinger-Wilke, C., et al., 2011). However, these studies have notable limitations such as ethical concerns, limited availability of human tissue, and the inability to capture specific factors related to aging and DD (Huang, Y. C, et al., 2014). In order to overcome these limitations and achieve a comprehensive understanding of IVD degeneration, in silico models have been developed.

Finite element (FE) models have been instrumental in examining the biomechanical aspects of the IVD at tissue-level, such as tissue stresses and nutrient transport (Schmidt, H. et al., 2013; Malandrino, A., et al., 2011; Zhu, Q., et al., 2012; Huang, Y. C., et al., 2008). However, these models have primarily explored how mechanical loads influence nutrition and cellular responses in a top-down approach, neglecting the reciprocal relationship between nutrition and mechanical loads. To address this, a bottom-up approach is necessary, considering how nutrition affects mechanical behaviour. While at

cellular-level, a parallel-network approach (Baumgartner, L., et al., 2022) have demonstrated the influence of nutrition on cellular production rates, the impact of these cellular changes on disc mechanics at the tissue level remains unexplored. Bridging the cellular-level activity with tissue-level mechanics would provide valuable insights into the complex interplay between ECM changes, nutrition, and mechanical behaviour in DD. This integration might have the potential to improve our understanding of IVD degeneration and pave the way for the development of targeted interventions and treatments in the future.

1.2 Aim

The aim of this thesis is to study at tissue level how proteoglycan changes due to nutrition affects IVD mechanical response. The L4-L5 IVD mechano-transport 3D model developed by the Biomechanics and Mechanobiology team of BCN MedTech will be used and integrated with a novel initial fixed charge density formulation, joining cellular-level activity and tissue-level mechanics. Non-degenerated and degenerated tissue conditions will be evaluated, grade I and grade III in Pfirrmann classification system, respectively.

2 State of the art

2.1 Human spine

The human spine is a complex anatomic structure that serves as the fundamental support structure for the entire body. It performs multiple vital functions, such as shielding the spinal cord and nerves and providing structural support, enabling us to maintain an upright posture ((Understanding spinal anatomy: Overview of the spine, n.d.). The spine is composed of the solid vertebrae, the intervertebral disc, and the associated ligaments that hold multiple vertebrae in place while still allowing for movement. This assembly of two adjacent vertebrae, intervertebral disc, facet joints, and their associated ligaments form the functional spine unit (Shim., 2018).The spine has three primary divisions (Fig. 1): the cervical, the thoracic, and the lumbar spine.

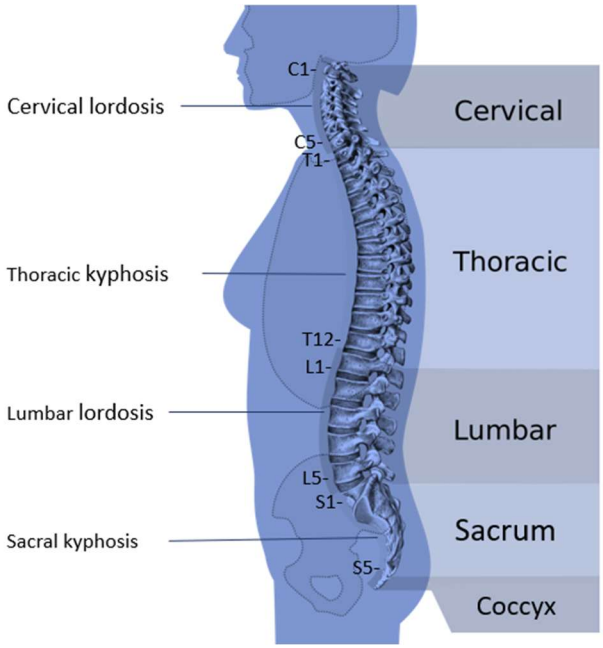

Figure 1. Adapted from (Spinal Curves: What is the ideal shape of the spine?, 2019)

Figure 1 illustrates the three primary divisions of the spine: The cervical region encompasses the upper part of the spine, comprising seven vertebrae identified as C1 to C7. The thoracic region occupies the middle segment of the spine and consists of 12 vertebrae, T1 to T12. The lumbar spine is the lower portion of the spine made up of five vertebrae, L1 to L5. Below the lumbar spine is the sacrum and coccyx.

2.2 Intervertebral disc structure

The intervertebral disc is a heterogeneous and fibrocartilaginous structure, composed of four distinct regions (figure 2): a central hydrated gelatinous core, the nucleus pulposus (NP) surrounded by the annulus fibrosus (AF), the transition zone (TZ) that connect both AF and NP, and the cartilage endplates (CEP) that confines the NP and the inner AF at the top and bottom of the disc. It functions to allow movement, acting as a shock absorber, transmitting loads, and providing flexibility to the spine (Oehme, D., 2022).

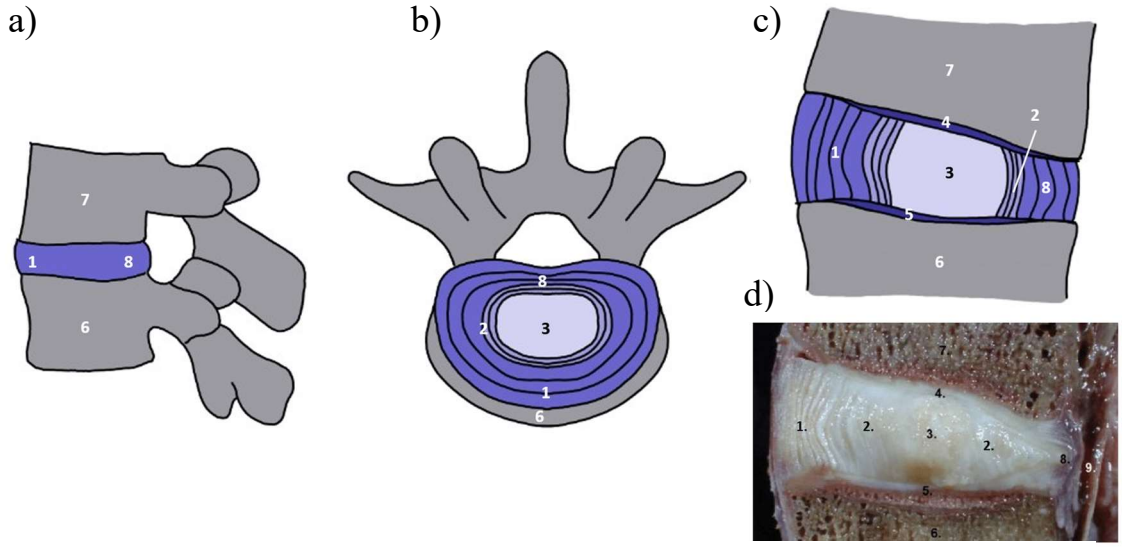

Figure 2. Intervertebral disc regions. Images a., b. and c. from own elaboration inspired from (Wikipedia-Intervertebral disc)., and d. modified image from (Melrose et al., 2016) corresponding to a vertical mid-sagittal section of adult human lumbar spine. 1. Anterior AF; 2. TZ; 3. NP; 4. Superior CEP; 5. Inferior CEP; 6. Inferior vertebral body (VB); 7. Superior VB; 8. Posterior AF; 9. Spinal canal.

Disc thickness generally increases from the upper (rostral) to the lower (caudal) regions of the spine. In the cervical and lumbar regions, the intervertebral discs are thicker towards the front (anteriorly), resulting in the formation of the cervical and lumbar lordosis, the secondary curvatures of the spine seen in figure 1 (Waxenbaum JA., et al., 2022). The variation in disc thickness along the spine is crucial as it influences the ability of the intervertebral discs to withstand high loads. Specifically, the thicker discs in the cervical and lumbar regions are essential for accommodating the increased range of motion and load-bearing requirements of these areas (Lumen Learning & OpenStax, n.d.) Consequently, the L4-L5 disc, located in the lumbar region, is particularly susceptible to injury and degeneration. This susceptibility arises from the significant stress it endures

and the challenges in nutrient diffusion caused by its relatively larger size. These factors contribute to the L4-5 disc's vulnerability to various spinal conditions including DD, spinal stenosis, disc herniation and disc bulge (Airrosti, 2022; Waxenbaum, J.A. et al., 2022; Donnally III, C.J. et al., 2023).

2.2.1 Annulus fibrosus

The annulus fibrosus is a fibrocartilaginous tissue consisting of a series of 15-25 concentric rings, or lamellae, with highly cross-linked collagen type I fibres lying parallel within each lamella and oriented at 28º to 43º to the vertical axis. This organization gives the annulus its functional anisotropic behaviour, especially under tension, axial rotation, and compression (Noailly et al. 2011). Therefore, the AF serves to provide structure to the gel-like NP and to allow effective resistance to multidirectional movements (Waxenbaum, J.A. et al., 2022; Physiopedia, n.d.).

2.2.2 Nucleus pulposus

The nucleus pulposus (NP) is the central gelatinous core of the disc. It contains a central region composed of loosely organized type II collagen and irregularly shaped radially organized elastin. These hold the gel-like area, which contains proteoglycan molecules (Raj P. P., 2008). The high concentration of proteoglycans confers osmotic properties, increasing the water content and contributing to the NP consistency. Moreover, this imbibition of water gives the nucleus its swelling capacity that allows the disc to resist compression load, recover from deformation and transmit loads radially to the annulus (Cramer, G. D., 2014).

2.2.3 Transition zone

The transition zone (TZ) consists in the interface between the AF and NP, where there is a gradual transition in structure, type of fibres and cells (Tavakoli & Tipper, 2022). It is characterized as the primary region within the disc for the synthesis of proteoglycans and proteins (Guilak et al. 1999; Chen, J., et al. 2002).

2.2.4 Cartilage endplate

The cartilage endplate (CEP) is a thin layer of hyaline cartilage that functions both as a mechanical barrier and as a gateway for nutrient transport into the disc (Moon, S. M., et al., 2013). It has approximately 1 mm thick horizontal layer of hyaline cartilage forming an important morphologically and functionally distinct junction between the annulus and the vertebral body (Raj P. P., 2008).

2.3 Extracellular matrix and biochemistry

The intervertebral disc (IVD) is constantly subjected to dynamic loads, which cause compressive, tensile, and shear stresses and strains on the cells embedded within its extracellular matrix (ECM) (Mainardi, A., 2022). The resistance to these forces is largely controlled by the ECM, which is composed mainly of water, collagen , and proteoglycans (Fig. 3). The ECM of the IVD is dynamic and undergoes continuous changes. The biochemistry and ultrastructure of the ECM regulate the mechanical properties of the disc, and the quality and integrity of the matrix are crucial to maintaining the disc's function and health (Vergroesen et al., 2015). Cellular processes within the disc regulate the synthesis and turnover of ECM components, such as collagen and proteoglycans, to maintain homeostasis (Shankar, H., et al., 2009).

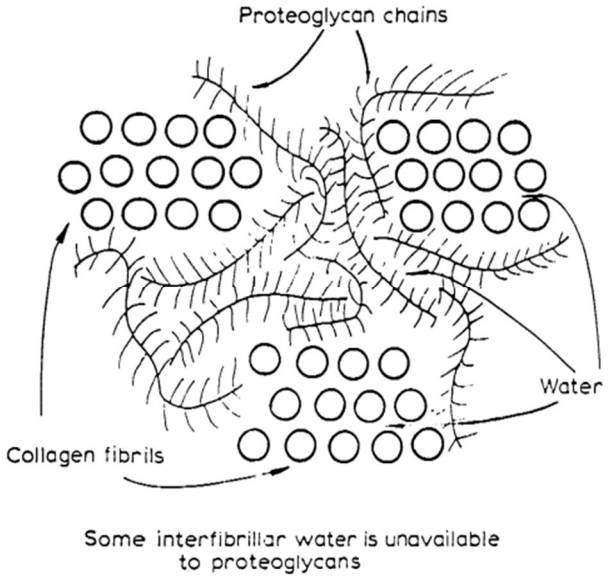

Figure 3. Scheme of the IVD ECM components (Urban, J. P., & McMullin, J. F., 1985).

2.3.1 Proteoglycans

Proteoglycans (PG) play a vital role in the IVD and are essential for its structure and function. Aggrecans are the main PGs in the IVD (Roberts & Urban 2011). They are mostly found in the NP, entrapped within the collagen type II fibres, and they consist of a protein core with glycosaminoglycan (GAG) chains attached. These chains contain negatively charged sulphated groups that attract small positively charged ions, creating a gradient of chemical potentials between the internal and external regions of the disc that results in water influx into the disc (Urban. et al., 1979). This is called the Donnan effect and allows the disc to swell, tensing the collagen fibres and leading to an intradiscal osmotic pressurization, which is essential for effective load distribution across the disc. Therefore, the dominant factor contributing to the osmotic pressure is not the PGs size, it is the ionic effect, so it is determined by the concentration of fixed negative charges present on the glycosaminoglycans (GAGs), specifically known as fixed charge density (FCD) (Urban, J. P., & McMullin, J. F., 1985). This swelling property helps maintaining disc height and biomechanical properties (Maroudas 1968; Huyghe et al. 2003). Moreover, through this effect PGs also play a role in regulating the movement of molecules through the disc matrix, influencing nutrient diffusion and waste removal (Urban & Roberts, 2003).

The NP has the highest content of proteoglycans, accounting for approximately 15% of its wet weight, while the Annulus Fibrosus (AF) and Cartilaginous Endplate (CEP) contain lower amounts (around 8% and 5%, respectively) (Urban & Roberts, 2011). This differential distribution reflects the specific functions and requirements of each region within the disc.

However, during disc degeneration, the content of proteoglycans decreases in all disc tissues (Singh, K., et al., 2009). This reduction can lead to diminished disc hydration, altered biomechanics, and compromised functionality. Understanding the half-life of proteoglycans is important for studying disc pathology and degeneration. Sivan et al.,

2006bhave shown that the half-life of proteoglycans in the NP is approximately 12±2 years.

2.3.2 Collagen fibres

Collagen fibres play a critical role in the IVD, with types I and II collagen being the primary forms present. Type I collagen is predominant in the AF, while type II collagen is found in higher concentrations in the NP (Zhang et al., 2022).

Within the AF, type I collagen forms highly oriented concentric lamellae. The arrangement of collagen fibres in successive lamellae with reversed orientations creates an organized structure giving the annulus its functional anisotropic behaviour (Holzapfel et al., 2005).

In the NP, collagen type II forms a network with a looser structure, enabling the absorption of water and maintaining disc height (Silver, F.H., et al., 2002). This extensible network allows for flexibility and helps dissipate loads within the disc. However, with degeneration or aging, there is an increase in the relative amount of collagen type I in the NP, leading to a shift in collagen composition. This, coupled with proteoglycan depletion, contributes to disc dehydration and a reduction in tissue porosity (Biyani et al., 2004; Antoniou, J. et al., 1996).

2.3.3 Water

Water is the main component of the IVD assuming between 65% and 90%, depending on age and area, of the total volume of the disc (Urban & Roberts, 2011). The intervertebral disc has an excellent swelling capacity to absorb water, which is thought to be largely due to the high proteoglycan amount. Therefore, the water content of the disc matrix is related to the amount of PG. In addition to being important for the mechanical functions of the disc, it is also of great importance for the transport of nutrients through the ECM (Urban & Roberts, 2011).).

In Fig 3., it can be seen that the PGs cannot penetrate into the collagen fibril; they are excluded from the intrafibrillar water (IFW) and confined to the extra-fibrillar space (Urban, J. P., & McMullin, J. F., 1985). Therefore, total amount of water is the sum of the IFW that fills the space between the collagen fibres (without PG) and the extrafibrillar water (EFW) that is the water in contact with PG. IFW is important in the annulus area, representing 30% of the fluid and EFW in the nucleus since it is proportional to the osmotic pressure (Sivan et al. 2006a)

2.4 Intervertebral disc mechanobiology

2.4.1 Nutrition of the disc

As the largest avascular tissue in the body, the IVD lacks direct blood supply to nourish its cells and maintain their function. Instead, nutrients essential for cellular activity, including glucose, oxygen, and matrix substrates, are primarily supplied by blood vessels located at the margins of the disc (Fig. 4) (Urban et al., 2004). While blood vessels around the annulus periphery provide nutrients to annulus cells, the nucleus and transition zone cells depend on a longer and precarious pathway from the blood vessels in the adjacent vertebral body for their nutrient supply and waste removal. To ensure the delivery of nutrients to the cells, diffusion plays a critical role. Disc cells consume oxygen and

glucose as they undergo metabolic processes, resulting in the production of lactic acid through glycolysis (Neidlinger-Wilke et al. 2012).

Maintaining a delicate balance between anabolic and catabolic processes is crucial for disc health. Anabolic processes involve the synthesis of matrix components and cellular maintenance, while catabolic processes involve the breakdown of matrix components. Disruption of this balance can lead to DD, with increased catabolic activity being a hallmark of disease progression (Gu, W., et al., 2014).

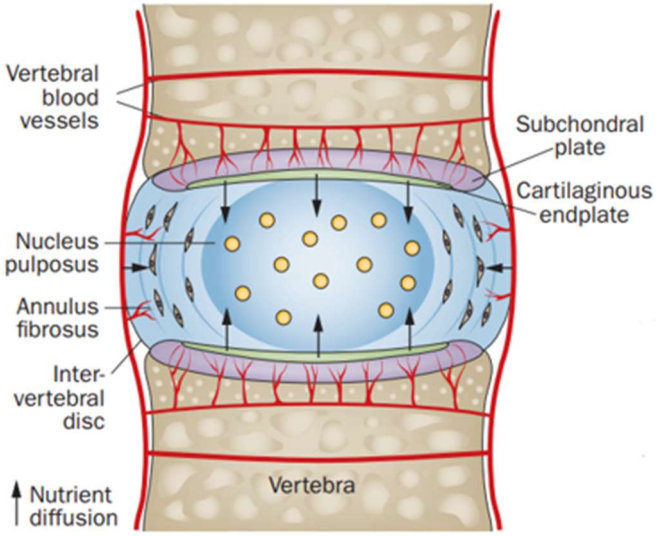

Figure 4. Pathways of nutrient supply in a normal intervertebral disc (Huang, Y. C., et al., 2014).

2.4.2 Disc cells

The IVD has a very low density of cells in comparison to other tissues; only 1% of the disc volume is occupied by cells (Urban & Roberts, 2011). The disc cell population consists of various cell types. Chondrocytes are present in the CEP, while fibroblast-like cells are found in the outer AF region. The NP cells of a mature human disc have a spherical shape similar to chondrocytes (Buckwalter, J.A, 1995). Despite their low number, these cells perform essential functions in maintaining the disc's ECM and overall health.

Cell viability is a critical aspect for maintaining a functional IVD. The precarious balance between nutrient supply and consumption within the disc is essential for the survival of these cells. Reduced nutrient transport can negatively impact cell viability, ECM integrity, and overall disc health (Jünger et al. 2009). The cells viability is influenced by factors such as glucose availability, pH levels, oxygen tension, osmolality, and mechanical loads (Sélard, É., et al., 2003; Soukane, D.M et. al., 2009). Horner & Urban (2001) study demonstrated that disc cells begin to die exponentially in the absence of glucose and under acidic pH conditions. Thus, a decline in nutrient transport into the disc can significantly impact cell viability, compromise the integrity of the disc's extracellular matrix, and contribute to DD.

2.5 Intervertebral disc degeneration

IVD degeneration is a complex process influenced by various factors. One significant cause is the disruption of nutrition to the disc cells (Urban & Roberts, 2003). This leads to a hostile environment that the cells are unable to support, losing the physiological response mechanisms that would maintain homeostasis (Vo, N. V., et al., 2016) and ultimately leading to their decay. Moreover, the lack of nutrient supply affects the cellular metabolism and triggers a series of catabolic cascades, such as the expression of matrix-degrading enzymes, contributing to the degenerative process (Vo, N. V., et al., 2016).

Disc degeneration is characterized by changes in the structure and function of the disc. The boundary between the AF and NP becomes less distinct, and the NP undergoes fibrotic changes, losing its gel-like properties (Fig. 5). This loss of tissue organization compromises the biomechanical function of the disc.

Figure 5. Normal and degenerated intervertebral disc. Left, is the normal disc where the annulus lamellae surrounding the NP is distinguishable. Right, is the degenerated disc where the annulus is disorganized, and the nucleus is desiccated (Urban & Roberts, 2003).

The depletion of proteoglycans is recognized as the most significant biochemical change occurring in disc degeneration. This loss of proteoglycans leads to a decrease in osmotic pressure, resulting in reduced water content within the disc. As a consequence, nutrient diffusion and mechanical response are compromised, causing the disc to struggle in maintaining hydration and resisting loads (Urban and Roberts, 2003).

To compensate for these changes, a shift in collagen expression takes place. Fine type II collagen fibrils in the inner annulus are replaced by coarser type I fibres (Biyani et al., 2004; Antoniou et al., 1996). Moreover, throughout the disc, type I fibres become coarser (Adams et al., 2006). Concurrent tissue fibrosis contributes to an increased relative amount of the solid phase at the expense of the fluid phase (Urban & Roberts, 2003); finally resulting in the collapse of the IVD.

2.5.1 Pfirmann grading system

The Pfirmann grading system is commonly used to classify degeneration in IVDs based on magnetic resonance imaging (MRI) findings. It provides a standardized approach to assess the severity of disc degeneration by evaluating the signal intensity, disc height, and distinction between the NP and the AF (Pfirmann et al., 2001) (Fig.6): grade I corresponds to a healthy disc, grade II to a disc with normal function but with loss of distinction between NP and AF, grade III represents a degenerated disc and a total loss of differentiation between NP and AF, grade IV presents fibrotic tissue and grade V a collapsed disc.

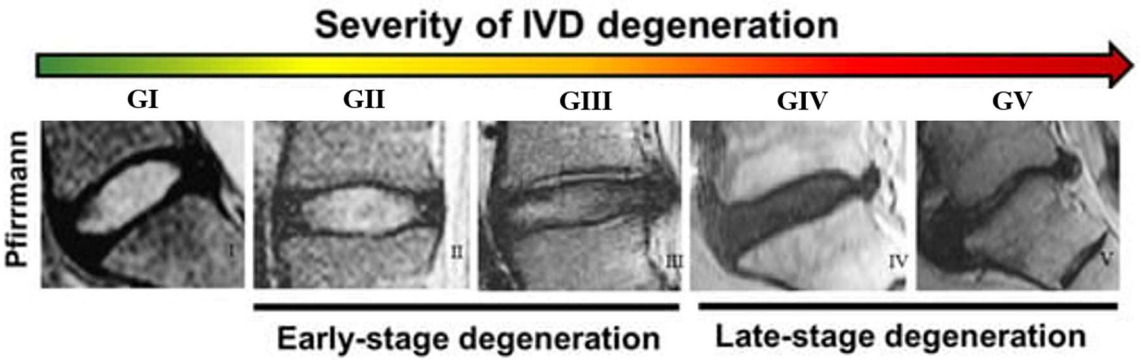

Figure 6. Pfirmann grading system (Ligorio, C. et al., 2022).

2.6 Approaches to study DD

Experimental studies have played a crucial role in investigating the ECM and cellular activities associated with DD. However, these studies have certain limitations: in vivo studies face challenges due to ethical considerations, limited control over variables, and difficulties in obtaining human samples. Ex vivo studies are constrained by the availability of human tissue and the inability to capture specific factors related to aging and degeneration. In vitro studies, although controlled, may not completely replicate the complex in vivo environment.

In silico models have emerged as valuable tools to complement experimental findings and enhance our understanding of DD. Finite element (FE) models and agent-based (AB) models are examples of such in silico models. FE offer valuable insights into the biomechanical aspects of the IVD, including tissue stresses and nutrient transport. On the other hand, AB models capture the intricate cellular interactions and biochemical processes occurring within the microenvironment of the disc. By integrating both types of models, researchers can gain a comprehensive understanding of IVD degeneration by being able to simulate various physiological and loading conditions and explore the effects on tissue behaviour without damaging specimens.

IVD tissues can be considered as biphasic materials, i.e., a combination of solid and liquid phases, at the millimetric scale. The solid phase represents the ECM, mainly composed of collagen and PG, while the liquid phase comprises water and solutes that flow through the pores within the solid phase.

Poroelastic models have been extensively employed to describe the time-dependent behaviour of disc tissues (Argoubi and Shirazi-Adl 1996; Natarajan and Andersson 1999). However, these models primarily focus on the mechanical aspects and do not consider the disc's biochemical composition. Iatridis et al. (2003) have shown that the influence of FCD on the mechanical behaviour of the tissue can be considered to model the disc. Additionally, as the disc undergoes aging and degeneration, the biochemical composition of its structural components undergoes changes (Adams et al. 1996), which impact the distribution of loads between the annulus and nucleus. This indicates a direct correlation between material properties and the tissue's biochemical composition (Adams et al. 1996). Therefore, the development of composition-based models became essential. Such models calculate the properties and mechanical response of different regions within the disc based on its specific biochemistry, primarily including water, collagen fibres, and

PG. Composition-based tissue model was developed for the articular cartilage (Wilson, W. et al., 2005) and was later applied to the IVD (Schroeder, Y., et al 2006), see Fig. 7.

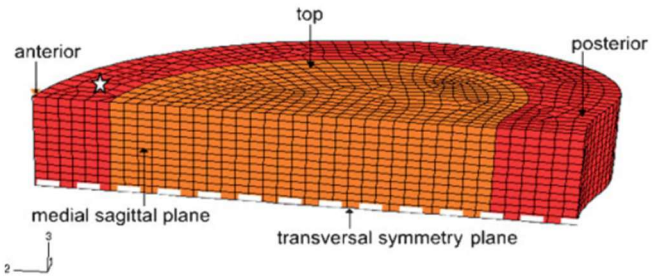

Figure 7. Schroeder et al. (2006) osmoporoviscoelastic FE mesh of ¼ IVD tissue model describing the annulus and nucleus tissue as a function of its biochemical composition and organization.

The impact of mechanically coupled solute transport on cellular activity in the intervertebral disc (IVD) is known as indirect mechanotransduction (Iatridis 2006). This phenomenon relies on the IVD tissues ability to deform and regulate factors such as diffusion distances and porosity, which relates to water content within the disc (Malandrino et al., 2011). In order to capture this mechanism, it is necessary to incorporate the description of anaerobic glycolysis. Bibby et al. (2005) conducted an experimental study that served as a basis for transport modeling. They investigated the metabolism of bovine nucleus cell cultures using electrochemical and biochemical sensors. The empirical equations derived from their findings have been integrated into metabolic transport models of the IVD (Huang, Y. C., et al., 2008; Malandrino A. et al., 2011; Q. Zhu 2012). These models incorporate standard diffusion-reaction. The integration of these equations allows for a more comprehensive understanding of solute distribution within the disc. Malandrino et al. (2011) found that mechanical loads and tissue properties might affect significantly the distribution of oxygen and lactate when large and prolonged volume changes are involved.

Cell viability was incorporated based on experimental studies (Bibby 2002, Horner 2001, Bibby 2004) assuming that cell density varies instantaneously with glucose concentration in IVD (Shirazi-Adl et al., 2010; Jackson et al., 2011). The absence of time-dependent cell death and the potential for cell revival when concentrations exceeded a threshold were significant limitations. However, Zhu et al. (2012) developed a novel constitutive model that introduced a rate of change in cell density based on the theoretical framework for microbial cell growth.

Ruiz Wills et al. (2016) coupled a 3D composition-based model with a transport model (Fig.8). The model included a osmo-poro-visco-hyperelastic formulation for disc tissues that considers the interaction between a hyperelastic porous matrix saturated with intra and extra-fibrillar fluid, a swelling pressure stress representing Donnan osmotic effects, and viscoelastic collagen fibres. Their results revealed that water contents in the disc, especially in the NP, largely control the effective diffusion of solutes, as well as the diffusion distances, under physiological mechanical loads.

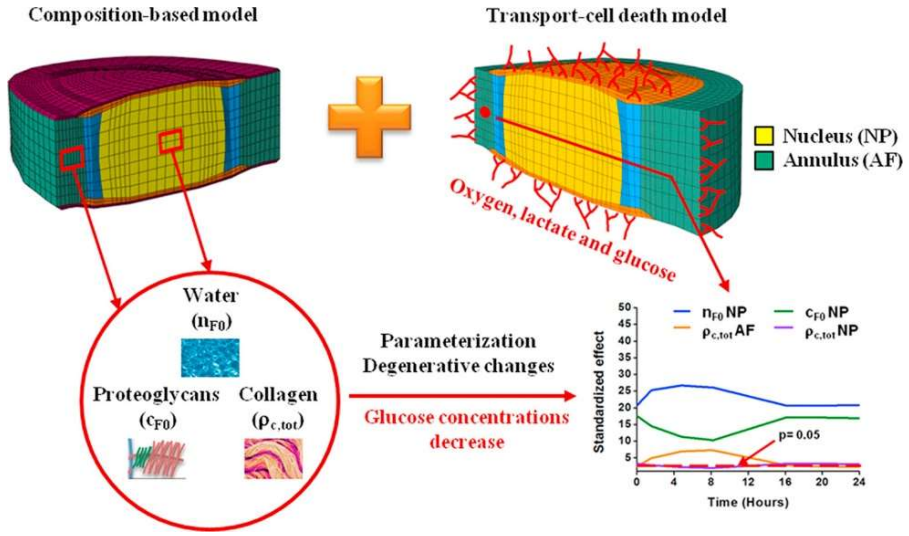

Figure 8. Composition-based and transport-cell death integration in a L4-L5 IVD 3D model (Ruiz Wills et al. (2016)).

Current FE used in IVD research predominantly take a top-down approach by focusing on how mechanical loads impact nutrition and cells within the disc. However, these models do not consider how changes in the ECM affect the mechanical response of the disc. At the cellular level, a novel agent-based model (Baumgartner, L. et al., 2022), combined with a top-down network modeling approach (time-dependent parallel network methodolofy, PNt-Methodology), was introduced to simulate the behaviour of NP cells within multicellular systems(Fig. 9). The model considered the influence of biochemical microenvironments. Integrating experimental data, such model can estimate cell viability and activity based on the relative expressions of specific mRNA markers, such as collagen types I and II, aggrecan, MMP-3, and ADAMTS proteases. Notably, this model has demonstrated that production rates are influenced by nutrition factors such as pH and glucose levels. However, the results are valid only for a small volume of tissue.

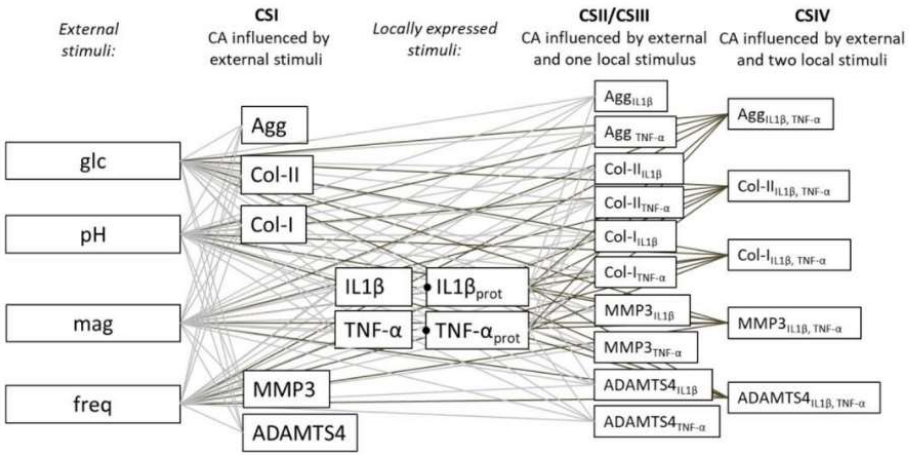

Figure 9. PNt-Methodology applied to approximate NP cell behaviour (Baumgartner, L. et al., 2022). The system involves four main external stimuli (glc, pH, mag, freq) that impact the cell activities (CA), which include the mRNA expressions of tissue proteins (Agg, Col-I, Col-II) and proteases (MMP3, ADAMTS4).

To gain a deeper understanding of how cellular changes affect the mechanical response of the intervertebral disc, a bottom-up approach needs to be done. This involves integrating the nutrition-dependent production rates obtained from the PNt-Methodology approach into tissue-level FE models. By doing so, researchers could explore the effects of alterations in the disc ECM on its mechanical behaviour.

3 Methodology

3.1 IVD 3D model

The current study utilized the generic L4-L5 IVD 3D Finite Element model, coupled with a transport-cell viability model developed by Ruiz et al. in 2016. This model incorporates anatomical regions such as the NP, AF, TZ and CEP, as well as a fixed surface representing the vertebral bodies known as the bony endplates (BEP) at the top and bottom. The model geometry present symmetry at the Sagittal plane, as such, only half model was used (Fig. 10).

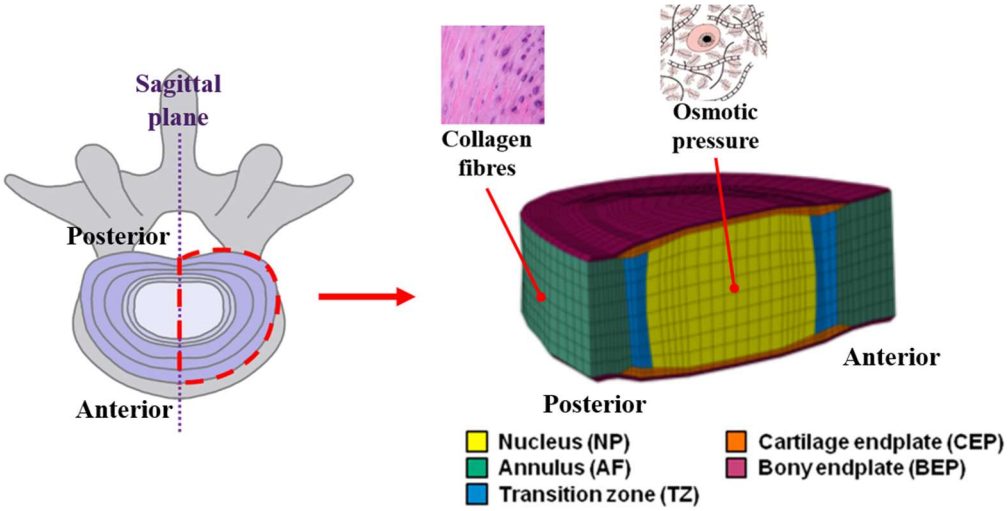

Figure 10. L4-L5 finite element disc 3D model with all sub-tissues adapted from Ruiz Wills C., et al. (2016).

All disc tissues are treated as osmo-poro-visco-hyperelastic materials (biphasic). The total stress tensor, σ, (Eq.1) is the combination of the stress tensor of the fluid and solid parts. The stress tensor of the porous solid skeleton (σ_{eff}) and the pore pressure component, p, (Eq. 2) contribute to the overall stress, which depends on the physical chemical potential of water (u_w) and the swelling pressure ($\Delta\pi$).

$$\sigma = \sigma_{eff} - pI \tag{1}$$

$$p = u_w + \Delta\pi \tag{2}$$

A modified neo-Hookean model is employed for the solid matrix (Schroeder et al., 2008). The model incorporates parameters such as the initial shear modulus (G_m), initial solid fraction ($n_{s,0}$), determinant of the strain gradient tensor (J), and first invariant of the left Cauchy-Green strain tensor (I).

The osmotic pressure gradient ($\Delta\pi$) is defined by the equation provided (eq. 4), which considers internal and external osmotic coefficients (φ_{int} and φ_{ext}), internal and external activity coefficients (γint and γext), external salt concentration (C_{ext}), and extra-fibrillar

fixed charge density ($C_{F,exf}$). The latter determined based on the amount of negative charge, which depends on the extra-fibrillar water content (n_{exf}) and the normal fixed charge density per millilitre of the total fluid (C_F) (eq. 5).

$$\sigma_{eff} = -\frac{1}{6}\frac{\ln(J)}{J}\, G_m I\left[-1 + \frac{3\left(J + n_{s,0}\right)}{\left(-J + n_{s,0}\right)^2}\right] + \frac{G_m}{J}\left(B - J^{\frac{2}{3}} I\right) \tag{3}$$

$$\Delta\pi = \varphi_{int} RT\left(\sqrt{C_{F,exf}^2 + 4\left(\frac{\gamma_{ext}^{\pm}}{\gamma_{int}^{\pm}}\right)^2 C_{ext}^2}\right) - 2\varphi_{ext} RT\, C_{ext} \tag{4}$$

$$C_{F,exf} = \frac{n_f C_F}{n_{exf}} \tag{5}$$

The extra-fibrillar water content (Eq. 6) is defined as the difference between the total water fraction (n_f) and the amount of intrafibrillar water. The parameter φ_{Ci} represents the intrafibrillar water per collagen mass, while $\rho_{C,tot}$ is the collagen content relative to the total wet weight. Moreover, the hydraulic permeability, k, of the tissue (Eq. 7) is influenced by the extra-fibrillar water content (n_{exf}). It is determined by the parameter α, which represents the initial permeability at zero strain, and a positive constant M.

$$n_{exf} = n_f - \varphi_{Ci}\, \rho_{C,tot} \tag{6}$$

$$k = \alpha\left(1 - n_{exf}\right)^{-M} \tag{7}$$

Viscoelastic collagen fibres were present only in the AF and assumed to exhibit a unidirectional viscoelastic mechanical response, which was simulated using a Zener rheological model; adapted to account for finite strains by incorporating two nonlinear springs (Schroeder et al., 2007).

3.2 Transport model

The composition-based disc model was coupled with a solute transport cell-viability model (Ruiz Wills C., et al. 2016) that considers the diffusion and reaction of oxygen, lactate and glucose within the tissue (Eq. 8),

$$\frac{\partial}{\partial t}\begin{pmatrix} C_{O_2} \\ C_{lact} \\ C_{gluc} \end{pmatrix} - \begin{pmatrix} D_{O_2} & 0 & 0 \\ 0 & D_{lact} & 0 \\ 0 & 0 & D_{gluc} \end{pmatrix} \nabla^2 \begin{pmatrix} C_{O_2} \\ C_{lact} \\ C_{gluc} \end{pmatrix} = \begin{pmatrix} R_{O_2} \\ R_{lact} \\ R_{gluc} \end{pmatrix} \tag{8}$$

where C, D and R are the concentrations, tissue diffusion coefficients, and the reactions of each solute, respectively.

The model considers tissue deformation and water content, obtained from the mechanical model by linking them to the reactive transport of the solutes using Eq. 9, which integrates the changes in porosity induced by mechanical factors based on the poromechanical equations. The effective diffusivity of each solute in the tissue (D_{solute}) is determined by

relating it to the solute diffusivity in water (D_{water}) using the Mackie Meares model (Mackie and Meares, 1955).

$$D_{solute} = \left(\frac{n_f}{2 - n_f}\right)^2 D_{water}\, I \tag{9}$$

Regarding metabolic reactions, the model incorporates a set of reactions described by Bibby and colleagues (Bibby et al., 2005), where the rates of oxygen consumption (R_{O_2}), glucose consumption (R_{gluc}), and lactate production (R_{lact}) are expressed in kPa/h, nmol/(mLh) and nmol/(mLh), respectively. The pH level is related to the concentration of lactate (in nmol/mL) through expression in Eq. 13 (Mokhbi Soukane et al. 2009) which is a linearization of experimental results of pH decay with lactate accumulation (Bibby et al. 2005). In this expression, a constant $1/A = -11.11$ nmol/mL quantifies the change in pH per unit of lactate concentration.

$$R_{O_2} = -n_f \frac{7.28\rho_{cell}}{s_{O_2}} \left(\frac{C_{O_2}(pH - 4.95)}{1.46 + C_{O_2} + 4.03(pH - 4.95)}\right) \tag{10}$$

$$R_{lact} = \rho_{cell} \exp\left[-2.47 + 0.93pH + 0.16\, C_{O_2} - 0.0058\left(C_{O_2}\right)^2\right] \tag{11}$$

$$R_{gluc} = -\frac{1}{2} R_{lact} \tag{12}$$

$$pH = 7.4 + A \cdot C_{lact} \tag{13}$$

Cell density dynamics, $\rho_{cell,\ t}$, is given by equation 14, that represent an exponentially decay, based on the study of Horner & Urban (2001), with low levels of glucose and acid pH. To accurately capture the spatiotemporal patterns of cell death within the IVD, death rates for pH (α_{pH}) and glucose (α_{gluc}) were determined by fitting curves to the experimental data from Horner and Urban's study (2001). These rates were recently adjusted by the group. Specifically, α_{pH} is modeled as a constant value of $5.7x10^{-6}\ s^{-1}$, while α_{gluc} depends on the glucose concentration (C_{Gluc}) according to the expression in Eq. 15 (Zhu et al., 2012), where k is a correction factor equal to $1.5x10^{-7}$.

$$\rho_{cell,\ t} = \rho_{cell,\ t-1} \cdot e^{-(\alpha_{gluc} + \alpha_{pH}) \cdot \Delta t} \tag{14}$$

$$\alpha_{glucose} = k \cdot \left(\frac{C_{Gluc} - 0.5}{C_{Gluc} + 0.2} - \left|\frac{C_{Gluc} - 0.5}{C_{Gluc} + 0.2}\right|\right) \tag{15}$$

The criteria for determining cell viability, i.e., when Eq. 14 is activated, are based on previous studies (Bibby & Urban 2004), where exponential decay begins when the glucose concentration drops below 0.5 nmol/mL, the pH value falls below 6.78, or both glucose and pH are below their critical values.

3.3 Initial fixed charged density approach

The initial fixed charge density (c_{F0}) of the NP was updated inside the transport model. The total PG content was calculated by considering two components (Eq. 16): PG decay due to half-life and PG production where $c_{F0,t-1}$ represents the initial FCD of the previous

time increment, where $c_{F0,0}$ is the initial FCD applied to the tissue, see Table 1. Δt is the time increment in years, λ is the decay constant given by eq. 17 where $t_{1/2}$is the half-life of disc proteoglycans (12 ± 2 years according to Sivan et al. (2006b).

$$c_{F0} = 0.5\left(c_{F0,t-1} \cdot exp(-\lambda * \Delta t) + c_{F0,0} \cdot (\omega_{Agg} \cdot \Delta t + CF) \cdot Cell_{viability}\right) \quad (16)$$

$$\lambda = \frac{Ln(2)}{t_{1/2}} \quad (17)$$

The production term incorporates a correction factor CF (Eq. 18), $Cell_{viability}$ accounts for the fraction of cells alive, and ω_{Agg} is the production factor that follows the expression in Eq. 19 from parallel-network (PN) approach developed by Baumgartner et al. (2022).

$$CF = (1 - \omega_{Agg} \cdot \Delta t) \quad (18)$$

$$\frac{d\omega_{Agg}}{dt} = \left(\frac{1 + \theta_{gluc} + \theta_{pH}}{\theta_{gluc} + \theta_{pH}}\right)\left(\frac{\theta_{gluc} * X_{gluc} + \theta_{pH} * X_{pH}}{1 + \theta_{gluc} * X_{gluc} + \theta_{pH} * X_{pH}}\right) \quad (19)$$

The production factor in the PN approach involves a weight factor θ, with values of 0.01 for glucose and 1 for pH (Baumgartner et al., 2022). The sensitivity of cell activity, denoted as X, is determined by glucose and pH levels. For glucose follows Eq. 20, and for pH it is defined for 2 ranges of pH levels, as presented in equations 21 and 22.

$$X_{gluc} = \frac{exp(18 * gluc)}{exp(18 * gluc) + 3x10^4} \quad (20)$$

$$6.5 \leq pH \leq 6.892 \qquad X_{pH} = \frac{exp\left(68 * (pH - 6.5)\right)}{exp\left(68 * (pH - 6.5)\right) + 2x10^4} \quad (21)$$

$$6.892 < pH \leq 7.4 \qquad X_{pH} = \frac{-exp\left(32 * (pH - 6.5)\right)}{exp\left(32 * (pH - 6.5)\right) + 5.035x10^{12}} + 1 \quad (22)$$

3.4 Boundary conditions

The mechanical model simulation consists of 24-hours cycle of physiological loading. This cycle includes 8 hours of rest under 0.11 MPa and 16 hours of activity under 0.54 MPa pressure load, based on average daily activities of a standard individual (Wilke et al., 1999). These loads are applied to the upper BEP, while the lower BEP remains fixed. External pore pressure is assumed to be negligible.

Literature-based values (Malandrino et al., 2014) for concentrations of oxygen, lactate and glucose were applied at the CEPs and the AF surfaces as reported in Fig. 11. Such, surfaces represent the blood vessel.

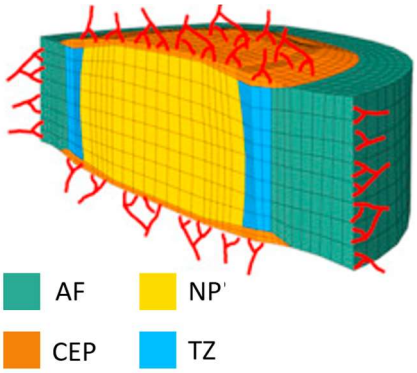

CEPs:
$C_{lactate}$=0.8 nmol/mL
C_{oxygen}=5.1 kPa
$C_{glucose}$=4 nmol/mL

AF:
$C_{lactate}$=0.8 nmol/mL
C_{oxygen}=5.1 kPa
$C_{glucose}$=4 nmol/mL

Figure 11. Solute boundary conditions applied at the surfaces of the AF and cartilage CEPs, image from Ruiz, et al. (2016).

As the FCD formulation is only valid for the NP, the analysis of the results was focus to this particular zone. Transport parameters examined were solute concentrations, cell viability and FCD. As for the mechanical parameters: intradiscal pressure (IDP), water content and height were considered. Both analyses were conducted along the mid-sagittal path and at three specific points: posterior, anterior, and centre NP. See Fig. 12 for a visual reference.

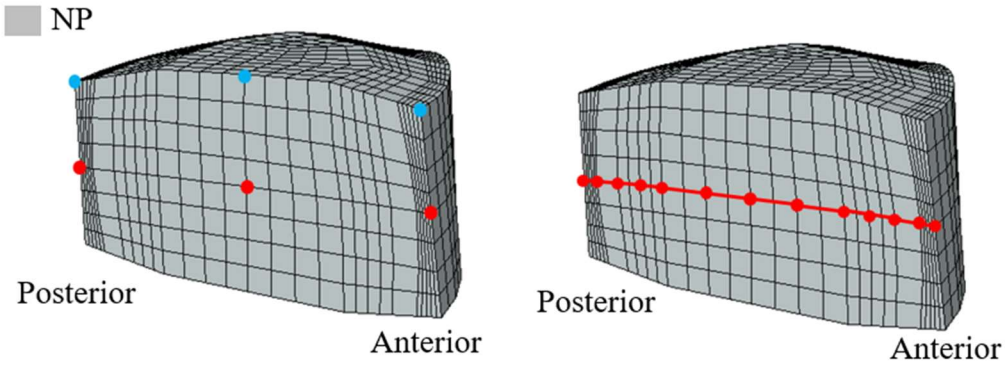

Figure 12. Regions for the analysis of results in the NP: node analysis (left) and mid-sagittal path (right). Blue nodes for the height assessment.

In the mechanics simulations, disc height was also evaluated within those regions by quantifying the vertical displacement. The measurements were taken for each simulation and region of interest (blue nodes in Fig. 12).

The material properties of the generic IVD model were consistent with those described in Ruiz Wills et al. (2018) (Table 1). The simulations involved changing the material properties of the CEP, AF, and NP to evaluate tissue conditions. All simulations were conducted using Abaqus 2018 (Dassault Systémés) in a Virtual Machine (Intel(R) Xeon(R) Silver 4210 CPU @ 2.20GHz).

Table 1. Material properties of IVD model tissues.

Tissue	NP		AF		CEP	
Grade	I	III	I	III	I	III
Matrix shear modulus (MPa)	1	0.8	1	0.7	1	0.8
Initial fixed charge density (mEq/mL)	0.30	0.23	0.20	0.20	0.17	0.13
Initial water content (% of wet weight)	80	76	75	70	66	60
Collagen content (% of dry weight)	15	28.5	65	78	24	35
External salt concentration (mEq/mL)	0.15	0.15	0.15	0.15	0.15	0.15
$\alpha(mm^4/Ns)$	0.00016	0.00045	0.00016	0.00045	0.0017	0.044
Constant M (-)	1.2	0.9	1.2	0.9	8.5	8.5

The PG evaluation consisted in simulating 14 years, that correspond to their half-lives. To achieve this, two stages of 7 years each were defined to establish two control points: the 7-year mark and the 14-year mark (see Fig. 13 for a schematic representation of the implemented simulations workflow):

- Stage 1, 7-year mark (7 years transport): initial FCD is updated by solute concentrations.
    - Mechanical simulation with stage 1 updated initial FCD and water content.
- Stage 2, 14-year mark (7 years transport): updated mechanical model is used for the stage 2 transport simulation. Initial FCD is updated with solute concentrations.
    - Mechanical simulation with updated stage 2 FCD and water content.

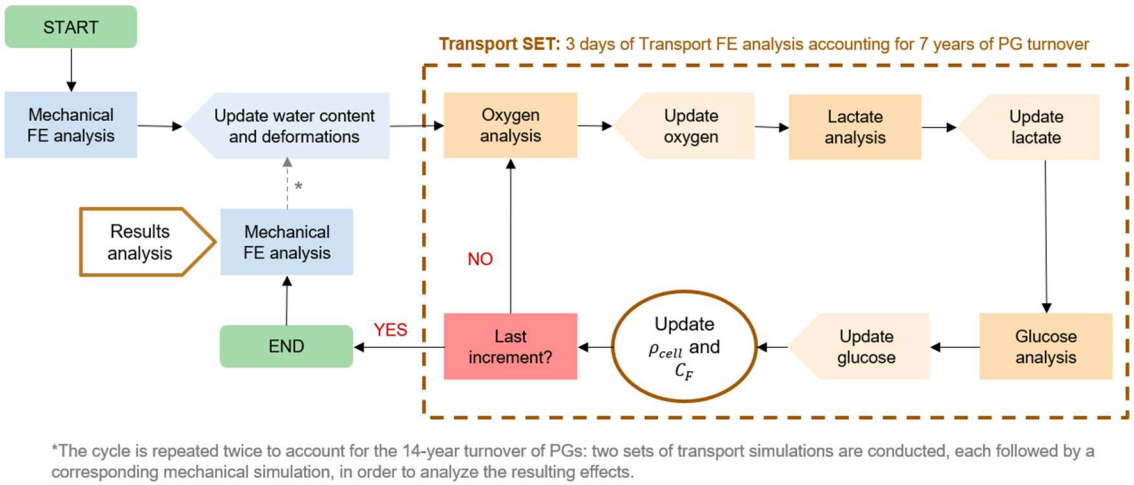

Figure 13. Scheme of the proposed model implementation for assessing the PG turnover i.e., 14 years.

Three scenarios were implemented to examine the turnover and production terms of the initial FCD formulation:

- Non-degenerated IVD (GI): solely the turnover term will affect the PG in a non-degenerated environment.
- Degenerated IVD with altered tissue properties but without considering cell death ($GIII_C$): solely the turnover term will affect the PG in a degenerated environment.
- Degenerated IVD (GIII), altered tissues properties and inclusion of cell death: effect of cell death in the outcome.

4 Results

4.1 Transport analysis

4.1.1 Solute concentrations

The concentrations of oxygen and glucose, and pH level were found to decrease when approaching anterior NP (Fig. 14). Consequently, the lowest concentrations were observed in the anterior NP region. In the case of GI, these values at the end of the simulation were 0.99 nmol/mL of glucose, 0.99 kPa of oxygen, and a pH of 6.91. In GIII, the values were 0.46 nmol/mL of glucose, 0.79 kPa of oxygen, and a pH of 6.84. Notably, the glucose concentration in this scenario fell below the viability threshold of 0.5 nmol/mL (Bibby et al., 2004). These findings are visually represented in Fig. 15, and specific values for each scenario at the 7-year mark can be found in Table 2, while those at the end of the 14-year simulation are presented in Table 3. Furthermore, a clear trend of decreasing solute concentration and pH towards the anterior NP and with progressive degeneration can be observed.

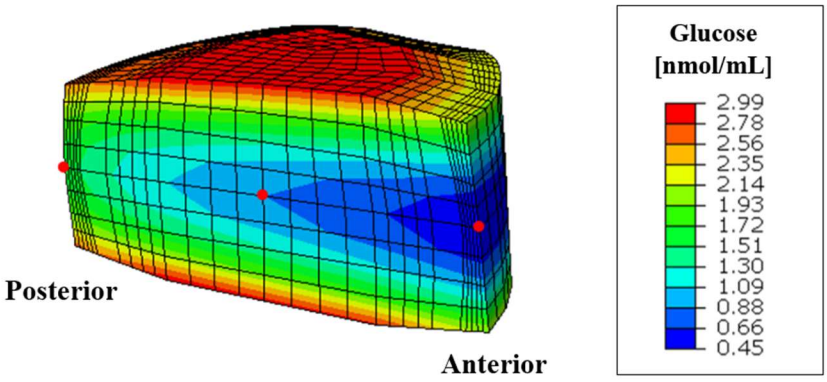

Figure 14. Distribution of glucose concentration [nmol/mL] in GIII IVD at the end of the 14-year simulation using a scale colormap. Nodes of analysis in the mid-sagittal path (posterior, centre, and anterior NP) highlighted in red.

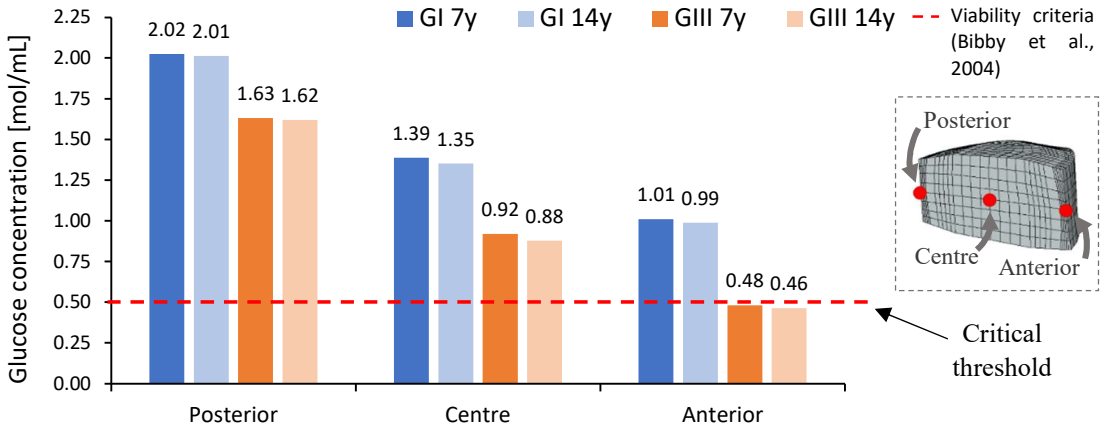

Figure 15. Glucose concentration [nmol/mL] at the middle and at the end of the 14-year transport simulation for non-degenerated (GI, blue) and degenerated (GIII, orange) IVD. Red dashed line represents the threshold of viability criteria (0.5 nmol/mL; Bibby et al., 2005)

Table 2. Oxygen [kPa], glucose [nmol/mL] concentrations and pH levels for the different scenarios and regions of study for the 7-year mark.

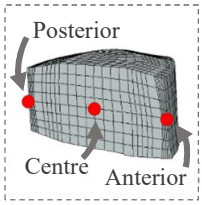

	Posterior			Centre			Anterior		
	O_2	pH	Glucose	O_2	pH	Glucose	O_2	pH	Glucose
GI	1.82	7.03	2.02	1.26	6.93	1.39	0.99	6.91	1.01
GIII	1.56	6.97	1.63	1.03	6.85	0.92	0.79	6.84	0.48

Table 3. Oxygen [kPa], glucose [nmol/mL] concentrations and pH levels for the different scenarios and regions of study at the end of the 14-year simulations.

	Posterior			Centre			Anterior		
	O_2	pH	Glucose	O_2	pH	Glucose	O_2	pH	Glucose
GI	1.82	7.02	2.01	1.25	6.92	1.35	0.99	6.91	0.99
GIII	1.56	6.97	1.62	1.01	6.84	0.88	0.79	6.84	0.46

4.1.2 Cell viability

Figure 2 illustrates the results of cell viability at the conclusion of the 14-year simulations. GI showed a 100% (Fig. 16a) of viable cells while in GIII a decreased cell density was observed in a specific region of the anterior NP (Fig. 16b) reaching a minimum of 89.99%. Table 4 provides the specific cell viability values obtained for this scenario.

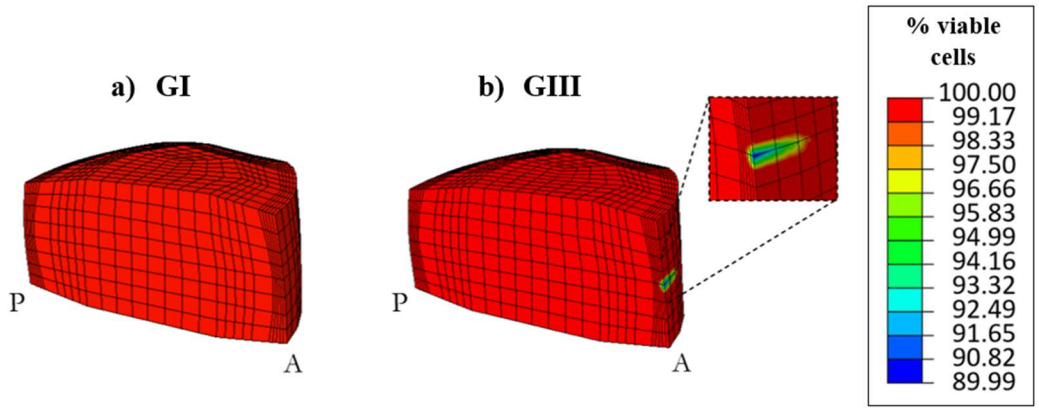

Figure 16. Cell viability [% viable cells] distribution using a scale colormap at the end of the 14-year simulations for a) GI and b) GIII. P and A stands for posterior and anterior regions, respectively.

Table 4. Cell viability [% viable cells] for GIII in the different times and regions of study.

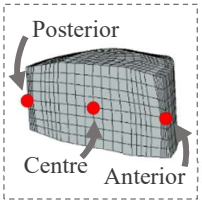

	NP region	initial	7 years	14 years
GIII	Centre & Posterior	100	100	100
	Anterior	100	99.75	89.99

4.1.3 Fixed charge density

At the end of the 14-year simulation, the FCD in GI and $GIII_C$ scenarios was found to be homogeneous. For GI, the FCD was determined to be 0.29536 mEq/mL, representing a 1.55% decrease from the initial value of 0.3 mEq/mL for the non-degenerated tissue. In the case of $GIII_C$, was 0.22655 mEq/mL, indicating a 1.51% decrease from the initial value of 0.23 mEq/mL for the degenerated tissue. In GIII, the overall FCD remained the same as $GIII_C$, except at the anterior region, where there is a significant drop of 11.45%, i.e. from 0.23 mEq/mL to a value of 0.20387 mEq/mL. These findings are visualized in Figure 17, and the specific values are provided in Table 5.

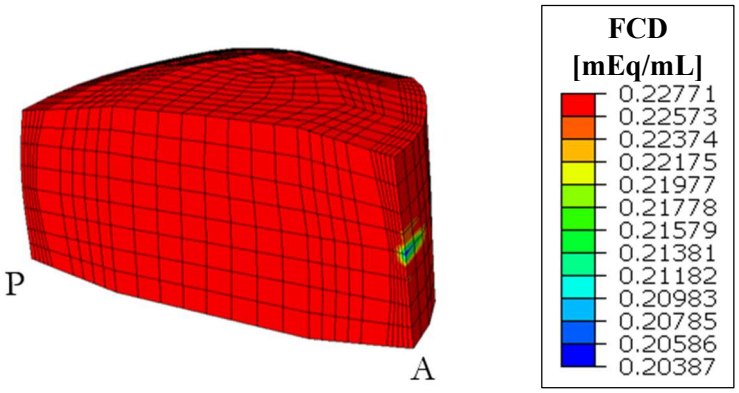

Figure 17. Fixed charged density, FCD [mEq/mL] distribution using a scale colormap at the end of the 14-year simulations for GIII IVD. P and A stands for posterior and anterior regions, respectively.

Table 5. Fixed charged density [mEq/mL] values for different scenarios, times of study and regions.

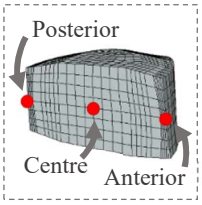

NP		initial	7 years	14 years	% decrease (14 years)
GI	Centre, Anterior & Posterior	0.3	0.29774	0.29536	1.55
$GIII_C$	Centre, Anterior & Posterior	0.23	0.22827	0.22655	1.51
GIII	Centre & Posterior	0.23	0.22827	0.22655	1.51
	Anterior	0.23	0.22799	0.20387	**11.45**

4.2 Mechanic analysis

4.2.1 Water content

The water content of the intervertebral disc exhibited a gradual decrease throughout the simulation period. In both GI and GIII tissue conditions, higher water content was observed in the posterior and anterior regions. Fig. 18 present the distribution of water content in the mid-sagittal path; in GI over the course of 7 years, there was an approximate 0.5% reduction in water content, followed by an additional 1% decrease in the subsequent 7 years. The initial water content ranged from approximately 77% to 78% of wet weight (ww) and decreased to 76% to 77% of ww at the end of the 14-year simulation.

For GIII the initial water content in the degenerated tissue ranged from 73% to 74% of ww. At the conclusion of the 14-year simulation, a total decrease of 14% in water content was observed, resulting in a range of 63% to 64% of ww. However, when not accounting for cell death, the reduction in water content was just for a 2%, ranging from 71% to 72%. After a 14-year simulation, the water content in GIII decreased by 18% compared to the same period in GI.

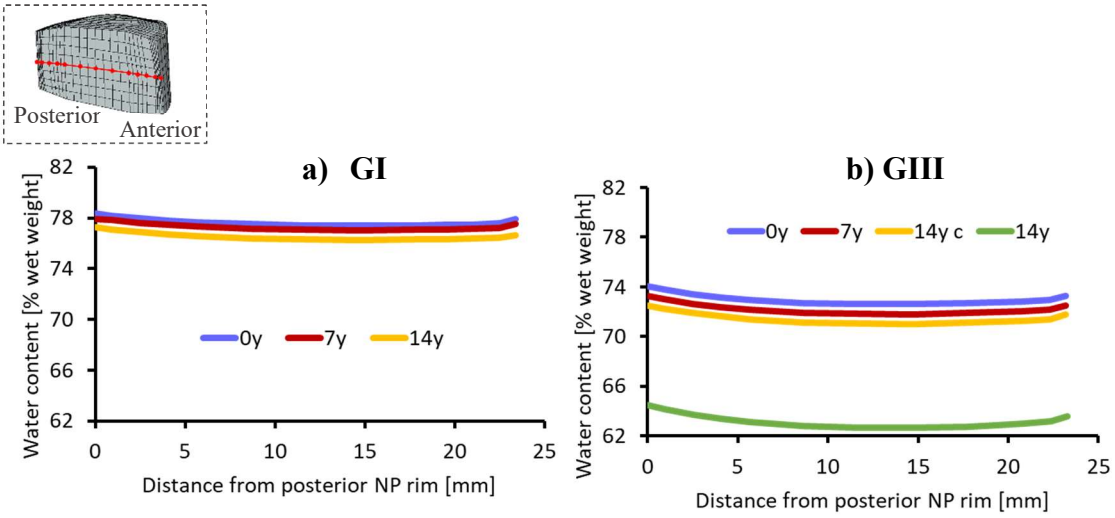

Figure 18. Water content [% wet weight] distribution along the mid-sagittal path for a) GI and b) GIII at different time points: Initial (0y), 7-year mark (7y), and 14-year mark (14y). "14y c" represents the GIII scenario without cell viability.

4.2.2 Intradiscal pressure

Figure 19 present the distribution of IDP along the mid-sagittal path of the NP for GI and GIII. In the GI scenario (Fig. 19a), the IDP demonstrates an increasing trend towards the anterior NP, while gradually decreasing over time. At the 7-year mark, a decrease of 2% is observed, while the subsequent 7 years show a less pronounced reduction of 0.1% for the centre and anterior NP regions. In contrast, the posterior NP experiences an almost 3% decrease. At the beginning of the 14-year period (0 years), the IDP ranged from 0.80 to 0.86 MPa and by the end (14 years), the range decreased to span from 0.75 to 0.84 MPa.

For GIII the distribution along the mid-sagittal path changes, showing an increased IDP in the centre and maintaining the posterior NP with the lowest IDP (Fig. 19b). Initially, the IDP ranged from 0.70 to 0.76 MPa. Similar to the Grade I scenario, the IDP decreased over time until the 7-year mark, showing a reduction of approximately 0.2% for the anterior and centre regions. However, for the subsequent 7 years, the IDP started to increase by 1.8% in these regions. Even when no accounting for cell death, there was still a slight increase of 0.2%. Ultimately, the IDP ranged from 0.70 to 0.78 MPa.

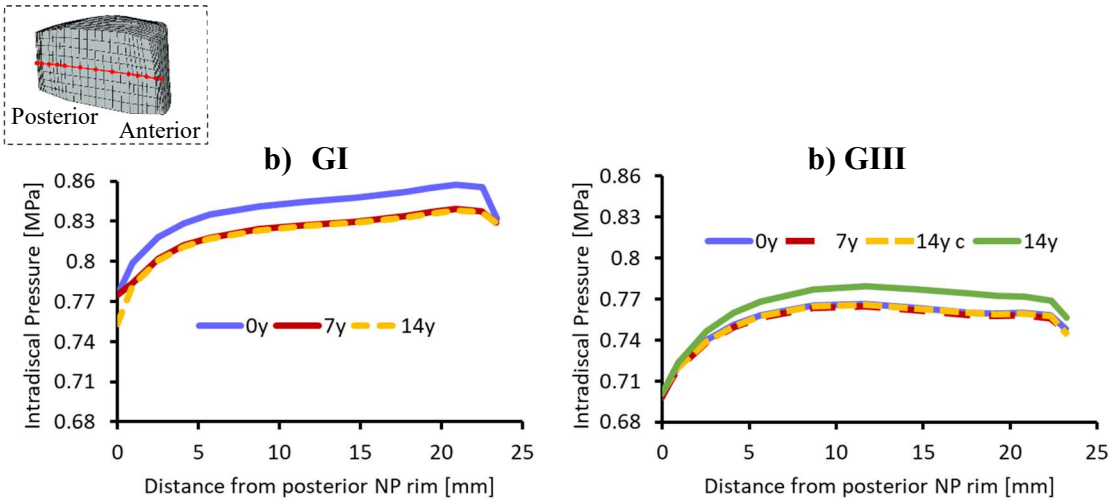

Figure 19. Intradiscal pressure distribution along the mid-sagittal path for a) GI and b) GIII at different time points: Initial (0y), 7-year mark (7y), and 14-year mark (14y). "14y c" represents the GIII scenario without cell viability.

4.2.3 Height

In GI, the posterior and anterior regions exhibited higher total displacements compared to the NP centre. However, in GIII, there was a shift in the displacement pattern, with the central region showing greater displacement than the anterior region. This distribution is visually depicted in Fig. 20 which displays the total displacements for the 14-year mark and highlights that GIII overall experiences higher total displacement. The total displacement remained relatively stable over time in both GI and GIII, as shown in Fig. 21. However, slight differences were observed in GIII at the 14-year mark, where the total displacement decreased by approximately 3 to 5% across all regions.

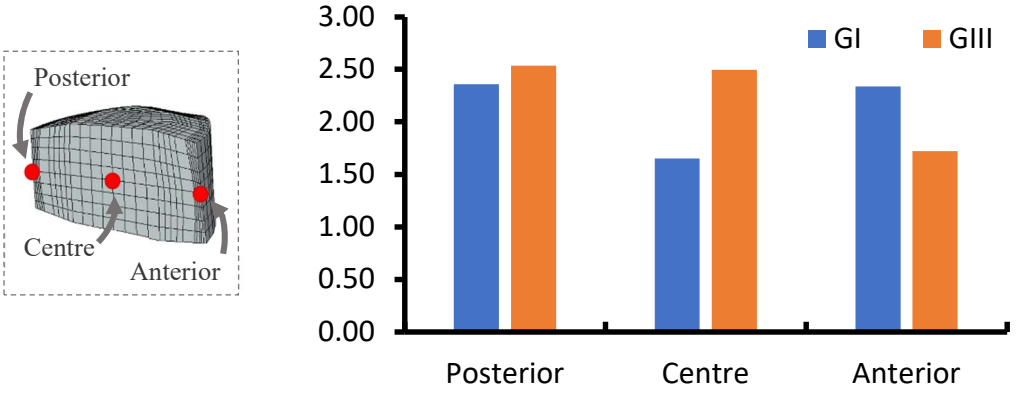

Figure 20. Total displacement for GI and GIII at the end of the simulation.

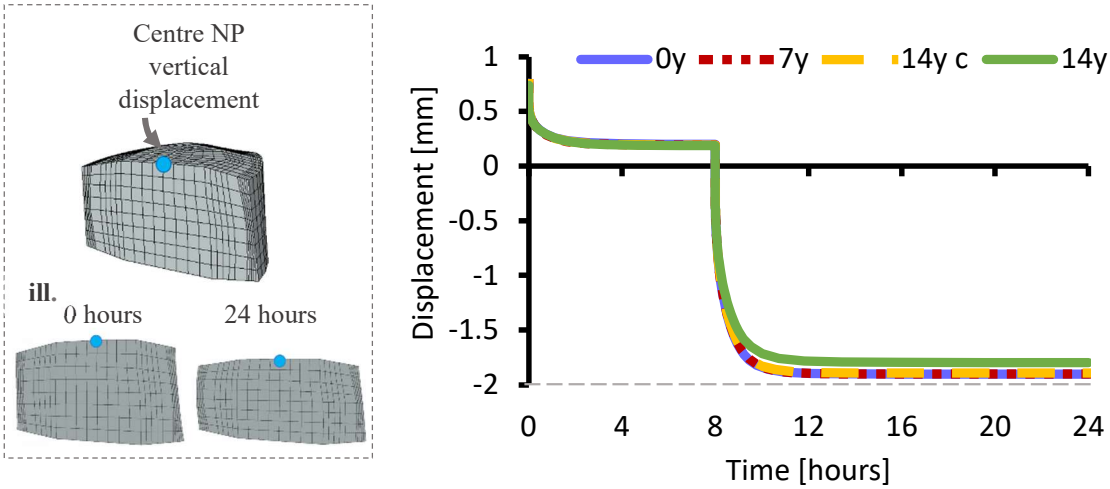

Figure 21. Comparison of the vertical displacement for GIII scenarios in time.

5 Discussion

Novel formulation of FCD has been included in a 3D L4-L5 mechano-transport IVD model with the aim to study the impact of PG changes due to nutrition on non-degenerated (GI) and degenerated (GIII) IVD mechanical response. To address this research problem, key parameters associated with DD were examined, including solute concentrations, water content, and fixed charge density. Such parameters were further evaluated in critical regions as the anterior nucleus TZ, known for its higher consolidation, and the central NP region where cells are exposed to adverse nutrient conditions due to prolonged diffusion distances, for a comprehensive understanding of the impact of PG alterations.

For the solute distribution, oxygen and glucose concentrations, and pH levels were found to decrease when approaching anterior NP (Fig. 14) as the distance from the nutrient supply increases. Solute concentrations and pH values barely change in GI simulation. In fact, between 7 years and 14 years the values remained almost unaltered. These results are consistent with what expect for a non-degenerate disc when the supplied is not altered by any other condition such a top and bottom endplate calcification. Also, for GI the fixed charge density decreased 1.5% at 14-year mark. The production term in Eq. 16, remained fully activate, since no cell death due to low concentration of glucose of pH level were observed. Baumgartner et al. (2020) reported that production of Aggrecans is full in

healthy nutritional environment (high values of glucose). Our results show a similar tendency. The reduction in fixed charge density obtained is related only with the half-life. This result suggests that production of aggrecans might attenuate the effect of the half-life. Such aspect needs to be confirmed experimentally.

On the other hand, in GIII condition the compromised environment showed a critical region in the anterior NP, where the glucose concentration falls below the critical viability threshold. Such glucose concentration reduction activated the cell viability, leading to a 10% of decrease in the cell density at the anterior NP. These findings suggest that the anterior NP region might experience higher concentrations of mechanical loads. This aspect agrees with MRI observation that reported inward bulging of annulus lamellae at the boundary AF-NP (Smith et al. 2011). Similar as GI, the GIII with no cell death (GIIIc) showed a decrease of 1.5% at 14-year simulation. Such results also show the attenuation effect that aggrecan production might have over the half-life. As for the grade III condition (GIII), a more substantial reduction of 11.5% in FCD was achieved at the anterior NP, where a reduction of cell density was observed. This emphasizes the significant influence of cell viability might have on FCD dynamics within the disc. In accordance with Baumgartner et al. (2020) study that reported a reduction of Aggrecans in a deprived nutritional environment, as there is a decrease in the cell density, the production of PG decrease contributing to the decrease of the FCD, being less able to attenuate the effect of half-life. This result suggests that if the reduction in cell density extends beyond the anterior region, it could potentially lead to a further decline in FCD throughout the disc. Gu et al., (2014) have reported that cell viability activation starts in the anterior NP-TZ and spreads to the central NP, emphasizing the importance of considering cell viability when studying disc degeneration.

During the 14-year simulation, the water content gradual decreased, with a higher decrease observed in the degenerated tissue. The values for GIII were lower than for GI. Water distribution along the mid-sagittal path (Fig. 18) in both GI and GIII showed a similar pattern, i.e., lower values at the centre and higher at the posterior and anterior NP zones. This distribution aligns with previous experimental and simulated findings (Iatridis, J. C., et al., 2007; Gu et al., 2014; Zhu, Q. et al., 2014) and indicates that the model simulates realistic distributions. Loading of the NP leads to swelling and the expulsion of water towards the periphery. This leads to an increase in water content in the outer regions of the NP (Costi, J. J et al., 2021). In addition, a previous study by Baldoni et al. (2019) found that reduction in FCD corresponds to a similar percentage reduction in water content. Our results for grade III indicate that in nucleus centre a 1.5% decrease in FCD corresponds to a 2% reduction in water content. At the anterior NP, a substantial decrease of 11.45 % in FCD showed a 14% decrease in water content. Highlighting the strong relation between PG loss and water dehydration. Furthermore, obtained values of FCD and water content are consistent with the measured by Urban & Maroudas (1979) reporting 0.28 mEq/mL for young disc (GI) and decreased to 0.20 mEq/mL for a degenerated disc, supposing an overall decrease of 19% of water content between both disc. Our results are similar, with 0.29536 mEq/mL in GI and 0.20387 mEq/mL in GIII, achieving a 18% of decrease in water content.

After 14 year the intradiscal pressure decrease in both GI and GIII disc (Fig.19). PGs generate an osmotic potential, which is translated into a biomechanical hydrostatic

pressure through the attraction of water. However, through degeneration, the increased fragmentation of aggrecan reduces its effective negative charge, which decreases IDP (Vergroesen, P.-P. et al., 2015). Interestingly, different IDP distribution is shown in GI and GIII (Fig.19). For GI, IDP increased towards the anterior NP, aligning with Zahari, S. N et al. (2017) study that highlights the effects of physiological loading in IDP in lumbar spine. The annulus of the disc acts as a containment structure, while the gel-like NP functions as a hydrostatic cushion that resists compressive forces and helps distributing loads. When a compression force is applied, the nucleus pulposus pushes more anteriorly due to the disc anatomical shape and the path of least resistance (Lumen Learning & OpenStax, n.d). This anterior displacement encounters resistance from the annulus, resulting in higher pressure in the anterior region.

The changes in IDP distribution along the mid-sagittal path for grade III disc might indicate alterations in pressure dynamics. The high IDP observed in the centre and anterior NP, with low IDP in the posterior, suggest changes in load-bearing and pressure distribution patterns due to the degenerative process. The differential response between the posterior and anterior/centre NP regions could be indicative of localized changes in tissue properties or load distribution within the disc. These findings might suggest an adaptive response or compensation mechanism within the degenerated disc aiming to maintain disc mechanical function. The subsequent observation of an increase in IDP after the first 7 years (Fig. 19b) is intriguing and could be explain because of the dehydration of the disc. The decrease in PGs leads to tissue dehydration and a reduction in the size of pores within the disc. This reduction in pore size can result in increased pressure exerted by the remaining PGs, as they occupy a smaller space and their interactions become more confined. Further research is needed for understanding the underlying mechanisms as there is currently lack of information.

As the intervertebral disc becomes less hydrated, its capacity to withstand compressive forces and retain its original height decreases over time (Urban & Roberts 2003). Consequently, degenerated tissue undergoes a larger total displacement compared to healthy tissue. Fig. 20 showed that the GIII disc has a higher total displacement than the GI disc. This result suggests that the degenerated tissue is not strong enough to bear the compressive load applied, and, in consequence, it deforms more. Such effect might be related to the fact that GIII disc has low fixed charge density, that reduces the osmotic pressure compromising tissue capacity to face compressive load.

In general, the overall displacement did not exhibit a significant decrease throughout the simulation (Fig. 21). This finding is consistent with the observations made by Zhu et al. (2014), indicating that disc height slightly decreases in mildly degenerated discs but is predicted to be noticeably in moderately degenerated discs. This suggests that for the simulated conditions and time, the decrease in FCD does not imply a significant change in height. However, this study provides insights into early indications of degeneration and possible critical regions, as the anterior nucleus. It is important to understand that disc degeneration is a progressive irreversible phenomenon (Hemanta, D., et al., 2016) characterized by the activation of a cascade of changes. This means that analysing the first indications is essential to understand the future progression and long-term implications on biochemical and structural changes. Providing a broader perspective of

possible more pronounced effects, for example when considering nutrient deprivation due to calcification or spread decrease in cell density in a moderately degenerated disc.

The sustained compression loads applied during the mechanical simulation contribute to tissue consolidation, particularly in the nucleus of the disc (Wachtel et al., 1998; Zernia et al., 2006). However, as degeneration progresses, increased consolidation of the nucleus leads to lower permeability and dehydration (Gu and Yao 2003; Nimer et al. 2003), impeding water redistribution; reducing disc nutritional transport capacity as water content was identified as disc biochemical component that affects the most disc nutrition (Ruiz Wills C., et al., 2016). Moreover, the high consolidation in the anterior TZ, attributed to the decrease of porosity in the TZ region due to the lateral pressure on the AF by the expansion of the NP (Ruiz Wills, C., 2015) is suspected to cause the lower glucose content with respect to the nucleus. Consequently, the results showed critical glucose concentrations in the anterior NP region, which lead to local cell death. The observed adaptive response of IDP highlights disc attempts to preserve its function in the face of degeneration.

This study is the first FE study to specifically address the effect of proteoglycans changes on disc mechanics. By providing insights into the complex interplay between biochemical and structural changes in disc degeneration, our study contributes to our understanding of the implications for IVD mechanics. Consistent with previous research (Vergroesen et al., 2015), we can perceive disc degeneration as a vicious cycle, where the homeostasis of the disc depends on the interaction of cells, extracellular matrix, and biomechanical stress. Disruption of this balance might compromise the production of PG, resulting in a decline in osmotic pressure, compromising the disc's ability to maintain hydration and nutrient diffusion (Urban & Roberts, 2003) and increasing shear forces on the cells. Shear forces might further decrease PG production, resulting in progressive degeneration. Moreover, strategies for repair or regeneration of IVD are based on the premise that degeneration results from inappropriate cellular behaviour (Hugan et al., 2014). Therefore, adopting a bottom-up approach to investigate the impact of nutrition and cell activity on mechanical response is crucial.

Like any numerical study, the present work has some limitations. First, the use of a generic model rather than a patient-specific one. While patient-specific models would offer a more personalized approach, the complex nature of DD requires a broader understanding. Generic models play a crucial role in establishing foundational knowledge and paving the way for future personalized treatments and patient-specific modelling. Second, the analysis was focused on the NP region, neglecting other regions like the annulus fibrosus. Annulus ECM also contains proteoglycan, which might be affected by nutrition. Yet, it is reasonable to start with the NP since it has been reported that loss of proteoglycan in the nucleus is a critical biochemical change in disc degeneration (Urban & Roberts, 2003). Third, the lack of available experimental data for direct validation poses a challenge in assessing the model's accuracy. However, the formulated model prioritizes internal consistency and biological plausibility to ensure reliable predictions within the limitations of the available literature data. Four, several simplifications and assumptions were made in the model, such as assuming a uniform decrease in FCD across the NP. Future work should investigate localized changes in FCD and consider variations in nutrient supply. Additionally, only sustained compression loads were implemented,

despite the disc being subjected to different static and dynamic load variations throughout a regular day. However, studies have shown that sustained compression has the most significant effect on disc nutrition (Malandrino et al., 2011), justifying its consideration in the model. Finally, the model does not consider aging or the presence of degrading enzyme such as proteases, which might have a substantial impact on the degenerative process. Future investigations should incorporate these factors to gain a more comprehensive understanding of IVD degeneration.

Overall, this study represents a step forward by integrating cellular-level activity with tissue-level mechanics in a finite element model. The insights gained from the present work might be invaluable for further exploration, refinement, and the development of personalized treatments and patient-specific models, ultimately addressing the multifactorial nature of IVD degeneration.

6 Conclusion

This study presents a ground-breaking approach by incorporating a novel nutrition-dependent fixed charge density formulation into a 3D IVD FE model. Meanwhile proteoglycans change barely altered non-degenerated disc mechanics, mayor changes were observed for a grade III disc in term of water, disc height, and intradiscal pressure. PG loss might activate a compensatory mechanism to preserve disc mechanical function. Furthermore, the decrease in water content due to proteoglycan loss might induce tissue stiffness and hinder nutrient diffusion, ultimately influencing cellular behaviour and leading to local death. The modelling approach used might provide crucial insights regarding the interaction between nutrition, disc composition and mechanical response. Such information might guide clinicians to develop new strategies for patients suffering from low back pain and disc degeneration.

7 Future work

Moving forward, future research should aim to extend the simulation period to evaluate moderate degeneration, while considering additional factors such as aging and proteases. Exploring the effects of higher grades of degeneration and incorporating patient-specific data into the models would further enhance our understanding of individual variations and enable personalized approaches to managing disc degeneration. By delving deeper into the intricate interplay between cellular activity, mechanical response, and degenerative processes, we can continue advancing our knowledge and develop targeted interventions to mitigate the prevalence of low back pain.

References

Adams, M. A., & Roughley, P. J. (2006). What is intervertebral disc degeneration, and what causes it?. Spine, 31(18), 2151–2161. https://doi.org/10.1097/01.brs.0000231761.73859.2c

Adams, M. A., McNally, D. S., & Dolan, P. (1996). 'Stress' distributions inside intervertebral discs. The effects of age and degeneration. The Journal of bone and joint surgery. British volume, 78(6), 965–972. https://doi.org/10.1302/0301-620x78b6.1287

Admin. (2019). Spinal Curves: What is the ideal shape of the spine? Norwest Chiro. https://norwestchiro.co.nz/spinal-curves-ideal-shape

Antoniou, J., Steffen, T., Nelson, F., Winterbottom, N., Hollander, A.P., Poole, R.A., Aebi, M., Alini, M. (1996). The human lumbar intervertebral disc: evidence for changes in the biosynthesis and denaturation of the extracellular matrix with growth, maturation, ageing, and degeneration. Journal of Clinical Investigation, 98(4), 996-1003.

Baldoni, M., & Gu, W. (2019). Effect of fixed charge density on water content of IVD during bed rest: A numerical analysis. Medical engineering & physics, 70, 72–77. https://doi.org/10.1016/j.medengphy.2019.06.011

Baradaran Mahdavi, S., Riahi, R., Vahdatpour, B., & Kelishadi, R. (2021). Association between sedentary behavior and low back pain; A systematic review and meta-analysis. Health promotion perspectives, 11(4), 393–410. https://doi.org/10.34172/hpp.2021.50

Baumgartner, L., González Ballester, M. Á., & Noailly, J. (2022). The PNt-Methodology: a top-down network modelling approach to estimate dose- and time-dependent cell responses to complex multifactorial environments. En bioRxiv (p. 2022.08.08.503195). https://doi.org/10.1101/2022.08.08.503195

Baumgartner, L., Wuertz-Kozak, K., Le Maitre, C. L., Wignall, F., Richardson, S. M., Hoyland, J., Ruiz Wills, C., González Ballester, M. A., Neidlin, M., Alexopoulos, L. G., & Noailly, J. (2021). Multiscale Regulation of the Intervertebral Disc: Achievements in Experimental, In Silico, and Regenerative Research. International journal of molecular sciences, 22(2), 703. https://doi.org/10.3390/ijms22020703

Bibby, S. R., & Urban, J. P. (2004). Effect of nutrient deprivation on the viability of intervertebral disc cells. European spine journal : official publication of the European Spine Society, the European Spinal Deformity Society, and the European Section of the Cervical Spine Research Society, 13(8), 695–701. https://doi.org/10.1007/s00586-003-0616-x

Bibby, S. R., Jones, D. A., Ripley, R. M., & Urban, J. P. (2005). Metabolism of the intervertebral disc: effects of low levels of oxygen, glucose, and pH on rates of energy metabolism of bovine nucleus pulposus cells. Spine, 30(5), 487–496. https://doi.org/10.1097/01.brs.0000154619.38122.47

Buckwalter J. A. (1995). Aging and degeneration of the human intervertebral disc. Spine, 20(11), 1307–1314. https://doi.org/10.1097/00007632-199506000-00022

Chen, J., Baer, A. E., Paik, P. Y., Yan, W., & Setton, L. A. (2002). Matrix protein gene expression in intervertebral disc cells subjected to altered osmolarity. Biochemical and Biophysical Research Communications, 293(3), 932–938. https://doi.org/10.1016/S0006-291X(02)00314-5

Costi, J. J., Ledet, E. H., & O'Connell, G. D. (2021). Spine biomechanical testing methodologies: The controversy of consensus vs scientific evidence. JOR Spine, 4(1), e1138. https://doi.org/10.1002/jsp2.1138

Cramer, G. D. (2014). General Characteristics of the Spine. In Elsevier eBooks (pp. 15–64). https://doi.org/10.1016/b978-0-323-07954-9.00002-5

De Cicco FL, Camino Willhuber GO. Nucleus Pulposus Herniation (2022) https://www.ncbi.nlm.nih.gov/books/NBK542307/

Donnally, C. J., III., Hanna A, Varacallo M (2023, January 15). Lumbar Degenerative Disk Disease. StatPearls - NCBI Bookshelf. https://www.ncbi.nlm.nih.gov/books/NBK448134/

Feng, Y., Egan, B., & Wang, J. (2016). Genetic Factors in Intervertebral Disc Degeneration. Genes & diseases, 3(3), 178–185. https://doi.org/10.1016/j.gendis.2016.04.005

Gillian Lyons, S.M. Eisenstein, M.B.E. Sweet, Biochemical changes in intervertebral disc degeneration, Biochimica et Biophysica Acta (BBA) - General Subjects, Volume 673, 1981. https://doi.org/10.1016/0304-4165(81)90476-1

Gruber, H.E., Hanley Jr, E.N. (2002). Analysis of aging and degeneration of the human intervertebral disc. Comparison of surgical specimens with normal controls. Spine, 27(8), 799-807.

Gu, W. Y., & Yao, H. (2003). Effects of hydration and fixed charge density on fluid transport in charged hydrated soft tissues. Annals of Biomedical Engineering, 31(10), 1162–1170. https://doi.org/10.1114/1.1615576

Gu, W., Zhu, Q., Gao, X., & Brown, M. D. (2014). Simulation of the progression of intervertebral disc degeneration due to decreased nutritional supply. Spine, 39(24), E1411–E1417. https://doi.org/10.1097/BRS.0000000000000560

Guilak, F., Ting-Beall, H. P., Baer, A. E., Trickey, W. R., Erickson, G. R., & Setton, L. A. (1999). Viscoelastic Properties of Intervertebral Disc Cells. Spine, 24(23), 2475. doi:10.1097/00007632-199912010-00009

Hariharan Shankar, Jeremy A. Scarlett, Stephen E. Abram, Anatomy and pathophysiology of intervertebral disc disease, Techniques in Regional Anesthesia and Pain Management, Volume 13, Issue 2, 2009, https://doi.org/10.1053/j.trap.2009.05.001.

Hemanta, D., Jiang, X. X., Feng, Z. Z., Chen, Z. X., & Cao, Y. W. (2016). Etiology for Degenerative Disc Disease. Chinese medical sciences journal = Chung-kuo i hsueh k'o hsueh tsa chih, 31(3), 185–191. https://doi.org/10.1016/s1001-9294(16)30049-9

Herniated disc injuries: Causes, symptoms and treatment. (s/f). AIRROSTI., de https://www.airrosti.com/injuries-we-treat/disc-injury-herniated-disc/

Horner HA, Urban JP. 2001 Volvo Award Winner in Basic Science Studies: Effect of nutrient supply on the viability of cells from the nucleus pulposus of the intervertebral disc. Spine. 2001 Dec;26(23):2543-2549. https://doi.org/10.1097/00007632-200112010-00006

Hoy, D., Bain, C., Williams, G., March, L., Brooks, P., Blyth, F., Woolf, A., Vos, T., & Buchbinder, R. (2012). A systematic review of the global prevalence of low back pain. Arthritis and rheumatism, 64(6), 2028–2037. https://doi.org/10.1002/art.34347

Holzapfel, G. A., Schulze-Bauer, C. A., Feigl, G., & Regitnig, P. (2005). Single lamellar mechanics of the human lumbar anulus fibrosus. Biomechanics and modeling in mechanobiology, 3(3), 125–140. https://doi.org/10.1007/s10237-004-0053-8

Huang, Y. C., & Gu, W.Y., 2008. Effects of mechanical compression on metabolism and distribution of oxygen and lactate in intervertebral disc. Journal of Biomechanics, 41(6), pp.1184–1196. : http://www.ncbi.nlm.nih.gov/pubmed/18374341

Huang, Y. C., Urban, J. P., & Luk, K. D. (2014). Intervertebral disc regeneration: do nutrients lead the way?. Nature reviews. Rheumatology, 10(9), 561–566. https://doi.org/10.1038/nrrheum.2014.91

Iatridis, J. C., MacLean, J. J., O'Brien, M., & Stokes, I. A. (2007). Measurements of proteoglycan and water content distribution in human lumbar intervertebral discs. Spine, 32(14), 1493–1497. https://doi.org/10.1097/BRS.0b013e318067dd3f

Iatridis, J. C., Nicoll, S. B., Michalek, A. J., Walter, B. A., & Gupta, M. S. (2013). Role of biomechanics in intervertebral disc degeneration and regenerative therapies: what needs repairing in the disc and what are promising biomaterials for its repair? The Spine Journal: Official Journal of the North American Spine Society, 13(3), 243–262. https://doi.org/10.1016/j.spinee.2012.12.002

Information about spine and intervetebral disc anatomy. (s. f.). Dr David Oehme Melbourne Neurosurgeon. https://www.doneurosurgery.com/spine--disc-anatomy.html

Intervertebral Disc. Physiopedia. (s/f). https://www.physio-pedia.com/Intervertebral_disc

Jackson, A. R., Huang, C. Y., & Gu, W. Y. (2011). Effect of endplate calcification and mechanical deformation on the distribution of glucose in intervertebral disc: a 3D finite element study. Computer methods in biomechanics and biomedical engineering, 14(2), 195–204. https://doi.org/10.1080/10255842.2010.535815

Jünger, S. et al., 2009. Effect of limited nutrition on in situ intervertebral disc cells under simulated physiological loading. Spine, 34(12), pp.1264–1271. Available at: http://www.ncbi.nlm.nih.gov/pubmed/19455001

Ligorio, C.; Hoyland, J.A.; Saiani, A. Self-Assembling Peptide Hydrogels as Functional Tools to Tackle Intervertebral Disc Degeneration. Gels 2022, 8, 211. https://doi.org/10.3390/gels8040211

Lumen Learning, & OpenStax. (s/f). The vertebral column. Lumenlearning.com. Recuperado el 18 de junio de 2023, de https://courses.lumenlearning.com/suny-ap1/chapter/the-vertebral-column/

Mainardi, A., Cambria, E., Occhetta, P., Martin, I., Barbero, A., Schären, S., Mehrkens, A., & Krupkova, O. (2022). Intervertebral Disc-on-a-Chip as Advanced In Vitro Model for Mechanobiology Research and Drug Testing: A Review and Perspective. Frontiers in bioengineering and biotechnology, 9, 826867. https://doi.org/10.3389/fbioe.2021.826867

Malandrino, A., Noailly, J., & Lacroix, D. (2011). The effect of sustained compression on oxygen metabolic transport in the intervertebral disc decreases with degenerative changes. PLoS computational biology, 7(8), e1002112. https://doi.org/10.1371/journal.pcbi.1002112

Mattiuzzi C, Lippi G, Bovo C. Current epidemiology of low back pain. J Hosp Manag Health Policy 2020;4:15. https://doi.org/10.21037/jhmhp-20-17

Mokhbi Soukane, D., Shirazi-Adl, A. & Urban, J.P.G., 2009. Investigation of solute concentrations in a 3D model of intervertebral disc. European Spine Journal, 18(2), pp.254–262. Available at: http://www.ncbi.nlm.nih.gov/pubmed/19015897

Moon, S. M., Yoder, J. H., Wright, A. C., Smith, L. J., Vresilovic, E. J., & Elliott, D. M. (2013). Evaluation of intervertebral disc cartilaginous endplate structure using magnetic resonance imaging. https://doi.org/10.1007/s00586-013-2798-1

Neidlinger-Wilke, C. et al., 2012. Interactions of environmental conditions and mechanical loads have influence on matrix turnover by nucleus pulposus cells. Journal of orthopaedic research : official publication of the Orthopaedic Research Society, 30(1), pp.112–21. Available at: http://www.ncbi.nlm.nih.gov/pubmed/21674606

Nimer, E., Schneiderman, R., & Maroudas, A. (2003). Diffusion and partition of solutes in cartilage under static load. Biophysical chemistry, 106(2), 125–146. https://doi.org/10.1016/s0301-4622(03)00157-1

Noailly, J., Planell, J.A. & Lacroix, D., 2011. On the collagen criss-cross angles in the annuli fibrosi of lumbar spine finite element models. Biomechanics and Modeling in Mechanobiology, 10, pp.203–219. Available at: http://www.ncbi.nlm.nih.gov/pubmed/20532944

Pfirrmann, C. W., Metzdorf, A., Zanetti, M., Hodler, J., & Boos, N. (2001). Magnetic resonance classification of lumbar intervertebral disc degeneration. Spine, 26(17), 1873–1878. https://doi.org/10.1097/00007632-200109010-00011

Raj P. P. (2008). Intervertebral disc: anatomy-physiology-pathophysiology-treatment. Pain practice : the official journal of World Institute of Pain, 8(1), 18–44. https://doi.org/10.1111/j.1533-2500.2007.00171.x

Rajasekaran, S., Venkatadass, K., Naresh Babu, J., Ganesh, K., & Shetty, A. P. (2008). Pharmacological enhancement of disc diffusion and differentiation of healthy, ageing and degenerated discs. https://doi.org/10.1007/s00586-008-0645-6

Roberts, S. & Urban, J.P.G., 2011. Intervertebral discs. In Encyclopaedia of Occupational health and Safety. Geneva. Available at: http://www.ilocis.org/en/contilo1.html.

Roberts, S., Evans, H., Trivedi, J., Menage, J. (2006). Histology and pathology of the human intervertebral disc. Journal of Bone and Joint Surgery, 88(Suppl 2), 10-14.

Ruiz Wills C. et al. (2018) Theoretical explorations generate new hypotheses about the role of the cartilage endplate in early intervertebral disk degeneration. Front. Physiol., 9, 1–12.

Ruiz Wills, C., Malandrino, A., van Rijsbergen, M., Lacroix, D., Ito, K., & Noailly, J. (2016). Simulating the sensitivity of cell nutritive environment to composition changes within the intervertebral disc. Journal Of The Mechanics And Physics Of Solids, 90, 108-123. doi: 10.1016/j.jmps.2016.02.003

Ruiz, C. (2015). A computational study of intervertebral disc degeneration in relation to changes in regional tissue composition and disc nutrition. Doctoral Thesis. UPC. http://hdl.handle.net/10803/327028

Schroeder, Y., Wilson, W., Huyghe, J. M., & Baaijens, F. P. (2006). Osmoviscoelastic finite element model of the intervertebral disc. European spine journal : official publication of the European Spine Society, the European Spinal Deformity Society, and the European Section of the Cervical Spine Research Society, 15 Suppl 3(Suppl 3), S361–S371. https://doi.org/10.1007/s00586-006-0110-3

Sélard, É.; Shirazi-Adl, A.; Urban, J.P.G. Finite Element Study of Nutrient Diffusion in the Human Intervertebral Disc. Spine 2003, 28, 1945–1953.

Shim. (2018). The Functional Spine Unit. ShimSpine. https://www.shimspine.com/functional-spine-unit/

Shirazi-Adl, A., Taheri, M., & Urban, J. P. (2010). Analysis of cell viability in intervertebral disc: Effect of endplate permeability on cell population. Journal of biomechanics, 43(7), 1330–1336. https://doi.org/10.1016/j.jbiomech.2010.01.023

Silver, F.H.; Horvath, I.; Foran, D.J. Mechanical implications of the domain structure of fiber-forming collagens: Comparison of the molecular and fibrillar flexibilities of the α1-chains found in types I-III collagen. J. Theor. Biol. 2002, 216, 243–254.

Singh, K., Masuda, K., Thonar, E. J., An, H. S., & Cs-Szabo, G. (2009). Age-related changes in the extracellular matrix of nucleus pulposus and anulus fibrosus of human intervertebral disc. Spine, 34(1), 10–16. https://doi.org/10.1097/BRS.0b013e31818e5ddd

Sivan, S. et al., 2006a. Correlation of swelling pressure and intrafibrillar water in young and aged human intervertebral discs. Journal of orthopaedic research official publication of the Orthopaedic Research Society, 24(6), pp.1292–8. Available at: http://www.ncbi.nlm.nih.gov/pubmed/16649177.

Sivan, S., Tsitron, E., Wachtel, E., Roughley, P. J., Sakkee, N., Van Der Ham, F., DeGroot, J., Roberts, S., & Maroudas, A. (2006b). Aggrecan Turnover in Human Intervertebral Disc as Determined by the Racemization of Aspartic Acid. Journal of Biological Chemistry, 281(19), 13009–13014. https://doi.org/10.1074/jbc.m600296200

Smith, L. J., Nerurkar, N. L., Choi, K. S., Harfe, B. D., & Elliott, D. M. (2011). Degeneration and regeneration of the intervertebral disc: lessons from development. Disease models & mechanisms, 4(1), 31–41. https://doi.org/10.1242/dmm.006403

Soukane, D.M.; Shirazi-Adl, A.; Urban, J.P. Analysis of Nonlinear Coupled Diffusion of Oxygen and Lactic Acid in Intervertebral Discs. J. Biomech. Eng. 2005, 127, 1121–1126.

Tavakoli, J., & Tipper, J. L. (2022). Detailed mechanical characterization of the transition zone: New insight into the integration between the annulus and nucleus of the intervertebral disc. Acta Biomaterialia, 143, 87–99. https://doi.org/10.1016/j.actbio.2022.03.002

Understanding Spinal Anatomy: Overview of the Spine. (n.d.-b). https://www.coloradospineinstitute.com/education/anatomy/spine-overview/

Urban, J. P., Maroudas, A., Bayliss, M. T., & Dillon, J. (1979). Swelling pressures of proteoglycans at the concentrations found in cartilaginous tissues. Biorheology, 16(6), 447–464. https://doi.org/10.3233/bir-1979-16609

Urban, J. P., & McMullin, J. F. (1985). Swelling pressure of the inervertebral disc: influence of proteoglycan and collagen contents. Biorheology, 22(2), 145–157. https://doi.org/10.3233/bir-1985-22205

Urban, J. P., Smith, S., & Fairbank, J. C. (2004). Nutrition of the intervertebral disc. Spine, 29(23), 2700–2709. https://doi.org/10.1097/01.brs.0000146499.97948.52

Urban, J.P., Roberts, S. Degeneration of the intervertebral disc. Arthritis Res Ther 5, 120 (2003). https://doi.org/10.1186/ar629

Vergroesen, P.-P. A., Kingma, I., Emanuel, K. S., Hoogendoorn, R. J. W., Welting, T. J., van Royen, B. J., van Dieën, J. H., & Smit, T. H. (2015). Mechanics and biology in intervertebral disc degeneration: a vicious circle. Osteoarthritis and Cartilage, 23(7), 1057–1070. https://doi.org/10.1016/j.joca.2015.03.028

Vo, N. V., Hartman, R. A., Patil, P. R., Risbud, M. V., Kletsas, D., Iatridis, J. C., Hoyland, J. A., Le Maitre, C. L., Sowa, G. A., & Kang, J. D. (2016). Molecular mechanisms of biological aging in intervertebral discs. Journal of orthopaedic research : official publication of the Orthopaedic Research Society, 34(8), 1289–1306. https://doi.org/10.1002/jor.23195

Wachtel, E., & Maroudas, A. (1998). The effects of pH and ionic strength on intrafibrillar hydration in articular cartilage. Biochimica et biophysica acta, 1381(1), 37–48. https://doi.org/10.1016/s0304-4165(97)00158-x

Waxenbaum, J. A, Reddy V, Futterman B. (2022). Anatomy, Back, Intervertebral Discs. StatPearls - NCBI Bookshelf. https://www.ncbi.nlm.nih.gov/books/NBK470583/

Wilke, H.J. et al., 1999. New in vivo measurements of pressures in the intervertebral disc in daily life. Spine, 24(8), pp.755–62. Available at: http://www.ncbi.nlm.nih.gov/pubmed/10222525.

Zahari, S. N., Latif, M. J. A., Rahim, N. R. A., Kadir, M. R. A., & Kamarul, T. (2017). The effects of physiological biomechanical loading on intradiscal pressure and annulus

stress in lumbar spine: A finite element analysis. Journal of healthcare engineering, 2017, 1–8. https://doi.org/10.1155/2017/9618940

Zernia, G., & Huster, D. (2006). Collagen dynamics in articular cartilage under osmotic pressure. NMR in biomedicine, 19(8), 1010–1019. https://doi.org/10.1002/nbm.1061

Zhang, S., Liu, W., Chen, S., Wang, B., Wang, P., Hu, B., Lv, X., & Shao, Z. (2022). Extracellular matrix in intervertebral disc: basic and translational implications. Cell and Tissue Research, 390(1), 1–22. https://doi.org/10.1007/s00441-022-03662-5

Zhu, Q., Gao, X., Brown, M. D., Temple, H. T., & Gu, W. (2017). Simulation of water content distributions in degenerated human intervertebral discs. Journal of orthopaedic research : official publication of the Orthopaedic Research Society, 35(1), 147–153. https://doi.org/10.1002/jor.23284

Zhu, Q., Jackson, A. R., & Gu, W. Y. (2012). Cell viability in intervertebral disc under various nutritional and dynamic loading conditions: 3d finite element analysis. Journal of biomechanics, 45(16), 2769–2777. https://doi.org/10.1016/j.jbiomech.2012.08.044